AGU PUBLICATIONS

Reviews of Geophysics

REVIEW ARTICLE
10.1002/2017RG000588

Key Points:
- A detailed review of radiocarbon marine reservoir effect research and its applications is presented
- The influence of the global carbon cycle on marine radiocarbon ages is discussed
- Spatiotemporal variations in ocean radiocarbon concentration are discussed

Correspondence to:
E. Q. Alves,
qa.eduardo@gmail.com

Citation:
Alves, E. Q., Macario, K., Ascough, P., & Bronk Ramsey, C. (2018). The worldwide marine radiocarbon reservoir effect: Definitions, mechanisms, and prospects. *Reviews of Geophysics*, *56*, 278–305. https://doi.org/10.1002/2017RG000588

Received 1 SEP 2017
Accepted 11 FEB 2018
Accepted article online 16 FEB 2018
Published online 30 MAR 2018

The Worldwide Marine Radiocarbon Reservoir Effect: Definitions, Mechanisms, and Prospects

Eduardo Q. Alves[1], Kita Macario[2], Philippa Ascough[3], and Christopher Bronk Ramsey[1]

[1]Oxford Radiocarbon Accelerator Unit, University of Oxford, Oxford, UK, [2]Laboratório de Radiocarbono, Universidade Federal Fluminense, Niterói, Brazil, [3]AMS Laboratory, Scottish Universities Environmental Research Centre, East Kilbride, UK

Abstract When a carbon reservoir has a lower radiocarbon content than the atmosphere, this is referred to as a reservoir effect. This is expressed as an offset between the radiocarbon ages of samples from the two reservoirs at a single point in time. The marine reservoir effect (MRE) has been a major concern in the radiocarbon community, as it introduces an additional source of error that is often difficult to accurately quantify. For this reason, researchers are often reluctant to date marine material where they have another option. The influence of this phenomenon makes the study of the MRE important for a broad range of applications. The advent of Accelerator Mass Spectrometry (AMS) has reduced sample size requirements and increased measurement precision, in turn increasing the number of studies seeking to measure marine samples. These studies rely on overcoming the influence of the MRE on marine radiocarbon dates through the worldwide quantification of the local parameter ΔR, that is, the local variation from the global average MRE. Furthermore, the strong dependence on ocean dynamics makes the MRE a useful indicator for changes in oceanic circulation, carbon exchange between reservoirs, and the fate of atmospheric CO_2, all of which impact Earth's climate. This article explores data from the Marine Reservoir Database and reviews the place of natural radiocarbon in oceanic records, focusing on key questions (e.g., changes in ocean dynamics) that have been answered by MRE studies and on their application to different subjects.

1. A Brief Overview on ^{14}C Dating

Influenced by research on cosmogenic radiation interactions in the atmosphere (e.g., Bethe et al., 1940; Clarke & Korff, 1941; Korff, 1939; Korff & Clarke, 1942; Korff & Hamermesh, 1946; Montgomery & Montgomery, 1939), Libby (1946) postulated that living carbonaceous matter contains the three naturally occurring carbon isotopes: ^{12}C, ^{13}C, and ^{14}C (or *radiocarbon*). Soon thereafter, this was proved to be true (Anderson et al., 1947), leading to the development of the radiocarbon dating technique (Arnold & Libby, 1949; Libby et al., 1949). The revolution brought about by this breakthrough was profound, crossing interdisciplinary boundaries and extensively impacting archeology, geosciences and environmental sciences, ultimately motivating the establishment of several radiocarbon laboratories around the world. For complete discussions, the reader is referred to texts such as Gillespie (1984), Taylor (1987), Aitken (1990), and Taylor (1992). More recent papers such as Bronk Ramsey (2008), Hajdas (2008), and Hua (2009) also present comprehensive analyses on the topic.

1.1. Scientific Background

Knowledge of the origin and distribution of ^{14}C plays a fundamental role in the reliable application of the dating tool based on this radionuclide. Radiocarbon is formed by a variety of mechanisms (e.g., nuclear transformations (Price, 1989; Rose & Jones, 1984; Vorobyov et al., 1972) and nuclear reactions induced by different factors (Lal, 1988; Zito et al., 1980)) but its continuous production in the upper atmospheric layers, where the maximum rate is at approximately 15 km above sea level, has been found to be the most relevant source of ^{14}C on Earth (Lal & Peters, 1967; Lingenfelter, 1963). High-energy nucleons promote spallation interactions with atmospheric nuclei (Gosse & Phillips, 2001; Muzikar et al., 2003), generating further cascades of nuclear reactions and leading to the formation of thermal neutrons. These particles are absorbed by atmospheric atoms to form cosmogenic nuclides (Gosse & Phillips, 2001). Radiocarbon is by far the most important of those nuclides (Gosse & Phillips, 2001; Libby, 1946), forming at a global average rate of 2.02 atoms cm^{-2} s^{-1} (Masarik & Beer, 1999) mainly by the following reaction:

$$^{14}_{7}N + n -> ^{14}_{6}C + p \quad (1)$$

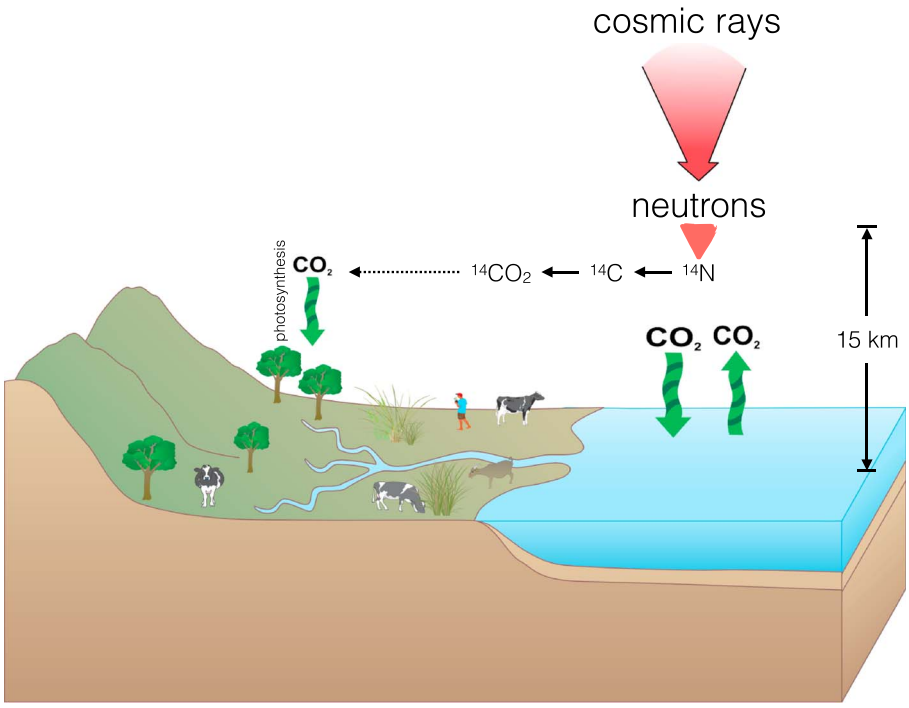

Figure 1. Simplified illustration of radiocarbon production, oxidation, absorption, and distribution throughout the Earth's reservoirs. Adapted from Aitken (1990). Some graphic elements are courtesy of the Integration and Application Network, University of Maryland Center for Environmental Science (http://ian.umces.edu/symbols/).

where n is a neutron and p is a proton. Newly formed carbon-14 atoms either directly form $^{14}CO_2$ or, most likely, rapidly produce ^{14}CO molecules (equation (2)) which undergo further oxidation by hydroxyl radicals, forming $^{14}CO_2$ (equation (3)) (Campbell et al., 1986; Pandow et al., 1960; Weinstock, 1969):

$$^{14}C + O_2 -> {}^{14}CO + O \tag{2}$$

$$^{14}CO + OH -> {}^{14}CO_2 + H \tag{3}$$

The chemical properties of these "heavy" carbon dioxide molecules are essentially identical to those of ordinary CO_2, and they are metabolically assimilated by primary producers via photosynthesis, reaching higher trophic levels via the food chain (Aitken, 1990). Atmospheric carbon dioxide also dissolves into the ocean and is taken up by the biota in this reservoir, as discussed in greater detail in section 4. Consequently, all living organisms are radioactive, incorporating ^{14}C but also the stable isotopes ^{12}C and ^{13}C (Figure 1). The biosphere maintains equilibrium with its supporting reservoir in a balance achieved by continuous assimilation of ^{14}C from the atmosphere and the counteracting process of radioactive decay:

$$^{14}_{6}C -> {}^{14}_{7}N + e^{-} + \bar{\nu}_e \tag{4}$$

where e^{-} is an electron and $\bar{\nu}_e$ is an electron antineutrino. Initial investigations by Craig (1953) revealed that equilibrium does not lead to the same radiocarbon activity. Indeed, biological systems usually exhibit isotopic ratios that differ from their supplier reservoir due to residence times and *isotopic fractionation*, a phenomenon caused by mass discrepancies between carbon isotopes affecting the uptake of molecules such as CO_2 in chemical and physical processes (e.g., photosynthesis). Following death, carbon exchange with the surrounding environment is suspended and organisms become sealed systems. Losses in radiocarbon content are then solely due to radioactive decay, occurring at a known rate, and the lack of replenishment (Figure 2). This closed system behavior lays the basis for the radiocarbon dating method, which can then be performed following the laws of radioactive decay. Provided that the initial ^{14}C activity is known and the current activity

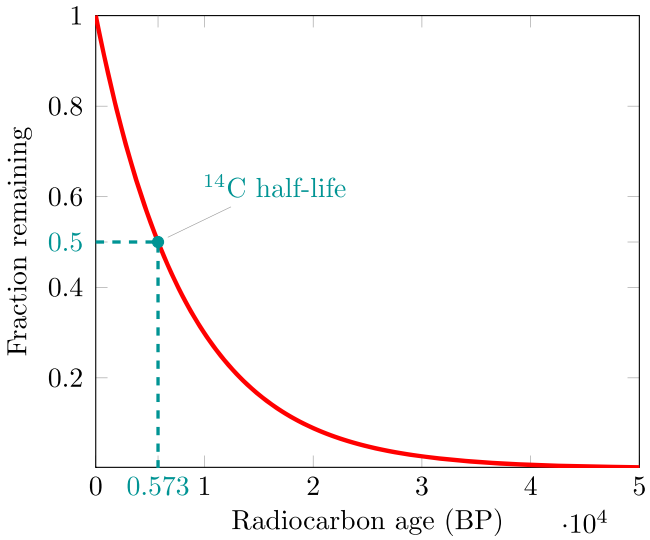

Figure 2. Radiocarbon decays to ^{14}N via β^- decay (equation (4)). Its convenient half-life (5,730 years) turns ^{14}C into a powerful clock for all sorts of processes happening in the Late Quaternary. After 10 half-lives, the quantity of residual radiocarbon is very low and the limit of the measurement technique is reached.

(or the concentrations) can be measured, one can calculate the elapsed time since the sample was removed from the exchangeable carbon reservoir, which is the *conventional radiocarbon age* of the sample:

$$t = -8033 \ln\left(\frac{A_{SN}}{A_{ON}}\right) \quad (5)$$

where A_{SN} is the isotopic fractionation corrected measured activity of the sample, A_{ON} is the fractionation corrected activity of the standard and 8033 is the Libby mean life of radiocarbon in years. It is important to highlight that the radiocarbon age is not an age in the usual sense of the word and the adoption of the above equation involves the following conventions and assumptions:

1. The use of 5568 years as the ^{14}C half-life.
2. The assumption that the atmospheric levels of ^{14}C were kept constant in the past.
3. The use of oxalic acid (directly or indirectly) as a standard.
4. Normalization of all sample activities to $\delta^{13}C = -25‰$ relative to the Pee Dee Belemnite (PDB) standard ($CaCO_3$ from *Belemnitella americana* (d'Orbigny, 1840) collected from the Peedee Formation of South Carolina, USA).
5. 1950 is the present, with all radiocarbon ages being given in years before 1950 AD.

The first two postulates do not hold but can be corrected when radiocarbon ages are translated into sidereal years through the use of a calibration curve (see section 2). For a complete discussion on the calculation of radiocarbon ages, the reader is referred to Stuiver and Polach (1977). This review does not cover all applications of natural and artificial ^{14}C measurements. The list is lengthy, ranging from archeology and global climate change to biomedical research. Examples of these and more applications, emphasizing the importance of the AMS technique for some studies, are discussed in publications such as Tuniz et al. (1998), Fifield (1999), Fifield (2004), and Hua (2009).

1.2. Experimental Methods

Techniques for the determination of isotopic ratios in a variety of materials have evolved, and technological advancements have led to methods of higher sensitivity and precision. Such techniques make use of beta particle detection (conventional method), direct counting of atoms, or even infrared absorption (Fifield, 1999; Povinec et al., 2009; Galli et al., 2011, respectively) to radiocarbon date a given sample.

Activity measurements employing either gas or liquid scintillation counters are the basis of the beta-counting techniques. These methods emerged with the development of the first gas counter, an instrument capable of counting electric pulses generated from the ionization of a gas by the emission of beta particles from the sample inside its chamber (Geiger & Müller, 1929). The possibility of measuring solid carbon samples arose when Libby (1934), aiming to study soft beta-emitters, developed a screenwall Geiger-Müller detector for solid materials. Nevertheless, these measurements were hindered by poor sensitivity and high backgrounds (Povinec et al., 2009). Given the low energy of ^{14}C beta-electrons, better precision was achieved in carbonaceous material measurements by replacing Libby counters with proportional gas counters (Povinec et al., 2009).

Almost simultaneously with the development of gas counters, Reynolds et al. (1950) worked with liquid scintillation equipment. For this approach, the sample must be converted to an organic solvent—commonly benzene due to advantages described in detail in Povinec et al. (2009) and references therein. In liquid scintillation techniques, an organic material, able to emit light, absorbs radiation and emits photons proportional to the number of received particles. These photons are then counted with the assistance of a photomultiplier.

These techniques share limitations. The amount of material necessary for the measurements is large (i.e., several grams C), making it impracticable to employ such methods for dating rare/scarce archeological material or in applications requiring submilligram samples. Moreover, the measurement time needed for achieving reasonable statistical precision is considerably long, this problem being worse for old samples whose activity is already diminished. For ^{14}C dating, it would be necessary to measure the activity of a sample of 1 g C

for 12 h to count 10,000 events and achieve 1% precision. For this reason, the application of beta-counting methods to radionuclides of long half-life is impractical. To overcome these limitations, a new method had to be developed.

Since the initial years of ^{14}C research, the possibility of counting atoms by mass spectrometry was a common suggestion (Olsson, 1970; Povinec et al., 2009). Although conventional mass spectrometers are able to separate carbon isotopes (^{14}C accounts for 0.0000000001% of atmospheric CO_2), they lack the energy required to resolve isobars. Intense fluxes of isobars (e.g., ^{14}N, ^{13}CH, $^{12}CH_2$, ^{12}CD, and $^{7}Li_2$) and background from the stable isotopes ^{12}C and ^{13}C mask ^{14}C ions (Fifield, 1999). In the late 1970s, the detection of ions with energies in the order of MeV was made possible by the coupling of particle accelerators developed for nuclear physics research with mass spectrometers (Muller, 1977). This means of counting individual atoms, named AMS, produces atomic and molecular ions from the sample that are then extracted and accelerated to high energies for the dissociation of molecular isobars and discrimination of isotopes according to momentum, charge, and energy. Soon after the articulation of the technique by Muller (1977), the first measurements of ^{14}C in natural materials using AMS were reported simultaneously by Nelson et al. (1977) and Bennett et al. (1977). Fifield (1999) summarized the significance of this technique for radiocarbon measurements observing that with AMS, the radiocarbon age of a sample less than 10,000 years old could be determined to a precision of 0.5% in a few minutes using a mg or less of carbon. Tuniz et al. (1998) pointed out that the revolution of AMS included long-lived radioactive nuclides, with the method applicable to many isotopes (e.g., ^{10}Be, ^{26}Al, ^{36}Cl, and ^{129}I). Traditional radiocarbon dating in fields such as archeology is no longer the only major application, and a review by Fifield (1999) covers the use of AMS in diverse fields including studies of atmospheric processes, ocean circulation, and past climates.

More recently, radiocarbon isotopic measurements have been performed by means of infrared absorption (Galli et al., 2011, 2013; Zare, 2012). After conversion to CO_2, infrared spectra are taken from the sample and carbon isotopes can be distinguished by differences in the absorbed frequencies. Using this method, in 1 h of averaging, Galli et al. (2011) measured $^{14}C/C$ ratios with an accuracy of 3.5%, approximately 1 order of magnitude worse than the best AMS uncertainty with the same acquisition time. Galli et al. (2013) present a comparison between this technique and both AMS and liquid scintillation counting for the measurement of radiocarbon concentrations. More recently, Galli et al. (2016) improved the performance of their technique using simpler and less expensive setup.

2. The Need for Calibration

Any attempt to use radiocarbon ages for calendrical time scale interpretations or comparisons with dates obtained by other methods would be problematic (Blockley & Housley, 2009; de Vries, 1958; Stuiver & Suess, 1966). The use of ^{14}C ages for chronological purposes assumes that the carbon isotopic concentration of the reservoir where the sample was formed has been constant (Stuiver & Suess, 1966). If this was indeed the case, then it would not be necessary to go any further than the result obtained by the application of equation (5) (provided that the correct ^{14}C half-life was used). However, the radiocarbon content of the Earth's reservoirs varies over time. The following paragraphs briefly discuss natural and anthropogenic reasons for calibration.

The geomagnetic field deflects low-energy charged particles (Muzikar et al., 2003), affecting the cutoff energies of cosmic rays (Lal & Jull, 2001; Masuda et al., 2009). The magnetic term of the Lorentz force requires this deflection to be strongest at low latitudes, where the velocity of incoming particles is perpendicular to the geomagnetic field (Muzikar et al., 2003). This creates a latitude dependence of the production rate of ^{14}C (Gosse & Phillips, 2001; Muzikar et al., 2003), which is enhanced at high latitudes where geomagnetic deflection is at a minimum. Altitude is also responsible for natural fluctuations in radiocarbon production rates. At approximately 15 km above Earth's surface, production of fast neutrons, density of target nuclei, and the number and energy of the cosmic radiation reach their maxima (Gosse & Phillips, 2001; Muzikar et al., 2003). This increases the likelihood of collisions between nitrogen and thermal neutrons, enabling a maximum in radiocarbon production.

The solar magnetic field also affects the trajectories of charged particles travelling through our solar system. It acts as a shield, inhibiting primary cosmic radiation from penetrating the Earth's atmosphere, playing an important role in the production of cosmogenic nuclides (Gosse & Phillips, 2001; Korff & Mendell, 1980; Muzikar et al., 2003; Stuiver et al., 1997). Stuiver (1961) was the first to observe that variations in radiocarbon

production rates are caused by solar wind modulating the interplanetary magnetic field. Sunspots have a higher magnetic field than the average field that is displayed by the Sun (Korff & Mendell, 1980; Tobias et al., 2004) and are a useful index for solar activity (Masuda et al., 2009). These features have been observed over the past several centuries, and the number of spots is inversely correlated with radiocarbon production rates (Masuda et al., 2009). Fluctuations in solar activity occur at different time scales and during the 11 year Schwabe cycles—caused by changes in the amplitude of the solar magnetic activity—^{14}C production rates in the minimum of solar activity reach 1.15 times the normal rate (Masarik & Beer, 1999). The long-term modulation of the solar magnetic activity (e.g., 210 year De Vries cycles and 2,300 year Hallstatt cycles) exhibits the same inverse proportional relation between cosmic radiation intensity and solar activity (Clilverd et al., 2003, 2004; Tobias et al., 2004). Finally, as Yamazaki and Oda (2002) point out, orbital influence on the Earth's magnetic field also leads to variation in solar irradiance and modulates radiocarbon production.

Rapid atmospheric mixing attenuates regional concentration differences caused by the latitudinal dependence of ^{14}C production. However, geographical offsets in radiocarbon concentration do persist. The most important of those refers to the offset between the two hemispheres as divided by the thermal equator (Hogg et al., 2011, 2013; McCormac et al., 2002). Lerman et al. (1970) demonstrated the interhemispheric offset via radiocarbon measurements of contemporaneous wood from the Southern and Northern Hemispheres. Their findings indicated that southern samples are older by approximately 30 ^{14}C yr. Other estimates have been made (McCormac et al., 1998; Stuiver & Braziunas, 1998; Vogel et al., 1993), and the offset is now known to vary temporally (Hogg et al., 2011; McCormac et al., 2002; Rodgers et al., 2011). The interhemispheric offset is considered to be a result of the larger oceanic area of the Southern Hemisphere, which increases the air-sea interface, enhancing CO_2 exchange fluxes (Hogg et al., 2011, 2013; Levin et al., 1987; McCormac et al., 2002). Indeed, this offset is attributed to the CO_2 exchange between the southern atmosphere and radiocarbon depleted surface waters in the upwelling zone of the circumpolar region (Levin et al., 1987). Fortunately, this discrepancy can easily be dealt with by using different atmospheric calibration curves for the different hemispheres (e.g., IntCal13 Reimer et al., 2013, and SHCal13 Hogg et al., 2013).

Volcanic eruptions can also impact radiocarbon concentrations as they release CO_2 devoid of ^{14}C into the atmosphere, lowering the radiocarbon content of plants nearby volcanic sites (Bruns et al., 1980; Sulerzhitzky, 1971). Volcanic influence is particularly relevant for samples younger than 10,000 years and may lead to apparent ages of up to 1,600 years (Bruns et al., 1980; Sulerzhitzky, 1971). Nevertheless, the effect of volcanic eruptions on the radiocarbon budget is very local, and negligible on a global scale.

Human interferences in the carbon cycle include the emission of ^{14}C-free CO_2 into the atmosphere through the combustion of ancient organic carbon molecules in domestic and industrial processes. The burning of coal, oil, and natural gas disturbs the carbon isotopic ratio of atmospheric CO_2 as first reported by Suess (1955). By measuring the carbon isotopic ratio of tree rings, Suess observed a dilution in the atmospheric ^{14}C concentration and associated changes in the stable isotopes content, which was termed the *industrial*, *fossil fuel*, or *Suess effect*. Efforts to quantify the Suess effect via the analysis of tree rings from the last two centuries revealed that wood grown in 1950 AD exhibits lower radiocarbon concentration than wood from 1850 AD (Stuiver & Quay, 1981; Suess, 1955; Tans et al., 1979). A spatial variation in the magnitude of the effect is also shown in the carbon records, with an enhanced Suess effect (i.e., lower than average reductions in radiocarbon concentration) registered in more polluted (Jong & Mook, 1982) and highly populated (Levin et al., 1989) areas. In addition, there is also a seasonal pattern, since fossil fuel CO_2 emissions intensify during the winter due to domestic heating, when the vertical mixing of the atmosphere is already reduced (Levin & Hesshaimer, 2000).

Another significant man-made perturbation in the global carbon budget is a consequence of nuclear tests in the 1950s and early 1960s. Over these years, some nations performed tests involving nuclear explosions in the atmosphere. Neutrons produced by these explosions eventually formed, in the same manner as for natural radiocarbon (equation (1)), 630×10^{26} or more atoms of what is called *bomb produced*, *artificial*, or *anthropogenic* ^{14}C (Hesshaimer et al., 1994). These large quantities of artificial radiocarbon caused a critical disequilibrium between the different reservoirs, doubling the atmospheric radiocarbon concentration in the Northern Hemisphere, where most explosions took place (Levin & Hesshaimer, 2000). This maximum in radiocarbon concentration in the Northern Hemisphere was reached in 1963 and in the same year nuclear tests were prohibited by the test ban treaty (Rakowski et al., 2005). Nevertheless, in the Southern Hemisphere the ^{14}C bomb peak was lower and occurred later, because it took time for the influence of the tests performed in the Northern Hemisphere to reach the Southern Hemisphere and wind patterns prevent a complete

interhemispheric mixing of the atmosphere (Hua et al., 2013). Since the ban of the tests, the bomb peak has been decreasing because of carbon exchange between the atmosphere and other reservoirs and the counteracting Suess effect (Broecker et al., 1985; Hesshaimer et al., 1994; Hua et al., 2013; Levin & Hesshaimer, 2000; Rakowski et al., 2005). This bomb pulse presents useful tracer properties, which allow the investigation of fluxes within the global carbon cycle (Hua et al., 2013; Levin & Hesshaimer, 2000).

Due to the reasons discussed above, the accuracy of the radiocarbon dating technique depends on highly refined calibration data. These data are used to account for temporal variations in the carbon isotopic ratios of reservoirs and to convert radiocarbon ages to calendar years using notations such as cal BP (Before Present, where 1950 AD is the present), cal CE (Common Era), cal BCE (Before Common Era), cal BC (Before Christ), and cal AD (Anno Domini). Terrestrial age calibration is performed in an empirical way, using curves of ^{14}C age versus calendar date constructed from the radiocarbon dating of known-age samples—mostly wood dated by dendrochronology (e.g., Pearson & Stuiver, 1993; Reimer et al., 2004, 2009, 2013; Stuiver, Reimer, & Braziunas, 1998; Stuiver, Reimer, Bard, et al., 1998). Atmospheric curves are mainly generated via radiocarbon measurements in annual growth rings from certain tree species (e.g., sequoias and oaks), with correspondent calendar years given by the counting of these rings. After formation, the wood deposited in these structures does not exchange carbon with the environment, reliably representing the atmospheric radiocarbon concentration in a particular year. The tree-ring approach yields accurate and high resolution data for radiocarbon calibration, being defined as the heart of the calibration process for the period 0–12.4 cal kyr (Blockley & Housley, 2009). Beyond this limit, samples such as foraminifera from varved sediments (Hughen et al., 2004), Th-U dated corals (Bard et al., 1998; Fairbanks et al., 2005), and speleothems (Southon et al., 2012) are incorporated to the calibration curves. However, radiocarbon ages from these samples must be corrected for reservoir effects to yield an equivalent terrestrial age, in a process much less straightforward than the tree-rings approach. Due to the lack of continuous highly resolved records, such as the tree rings mentioned above, in the marine environment (Stuiver & Braziunas, 1993), marine curves are generated with the aid of numerical models. Considering parameters involved in the uptake and distribution of carbon in the ocean, an ocean-atmosphere box diffusion model (Oeschger et al., 1975; Stuiver & Braziunas, 1993; Stuiver et al., 1986) estimates the oceanic response to fluctuations in atmospheric ^{14}C concentration. It is important to note that data constituting different sections of the marine calibration curve Marine13 are composed by the measurements of marine materials, modeled atmospheric data from IntCal13 or both (Reimer et al., 2013). Details on the construction of the last curves can be found in Hogg et al. (2013), Niu et al. (2013), and Reimer et al. (2013). Although radiocarbon dating is now consolidated as a valid and powerful technique, the correction using empirical data is a step that must be taken toward a calendar date. Complete discussions on the calibration of the radiocarbon time scale and its implications can be found in articles such as Bard (1998) and Damon and Peristykh (2000).

3. The Global Carbon Cycle: Reservoirs and Residence Times

Gigatons (Gt) of carbon flow between distinct reservoirs, at variable rates and states of matter, every year on Earth. The geological and environmental mechanisms of carbon exchange among reservoirs are collectively called the global carbon cycle, and the carbon held in the active reservoirs of atmosphere, biosphere, and sea was defined by Craig (1957) as the *exchangeable system*. The global carbon cycle can be defined as a biogeochemical cycle in which carbon is recycled and reused throughout the reservoirs (see Figure 3). The mass conservation principle guarantees that there are no losses and any shift in carbon content taking place in a reservoir affects the quantity of carbon in the others. For instance, considering the atmosphere-ocean system, the acidification of the world's oceans due to rising levels of atmospheric CO_2 (see, e.g., Doney et al., 2009) exemplifies the link between reservoirs. Activities such as deforestation and the burning of fossil fuels, which increase CO_2 input to the atmosphere with no matching increase in potential sinks for this CO_2, pushes the global carbon cycle out of equilibrium.

The magnitude of the atmospheric carbon reservoir has been accurately established since 1958 when Charles Keeling started measuring CO_2 concentrations at the Mauna Loa observatory in Hawaii (Post et al., 1990), demonstrating that the quantity of atmospheric CO_2 has been growing because of human activity. Indeed, due to anthropogenic perturbations to the carbon cycle, atmospheric CO_2 concentration is currently around 100 ppmv higher than in preindustrial times, having reached that level at a rate at least 10 times faster than at any other time in the 420,000 years before the Industrial Revolution (Falkowski et al., 2000). Apart from fossil

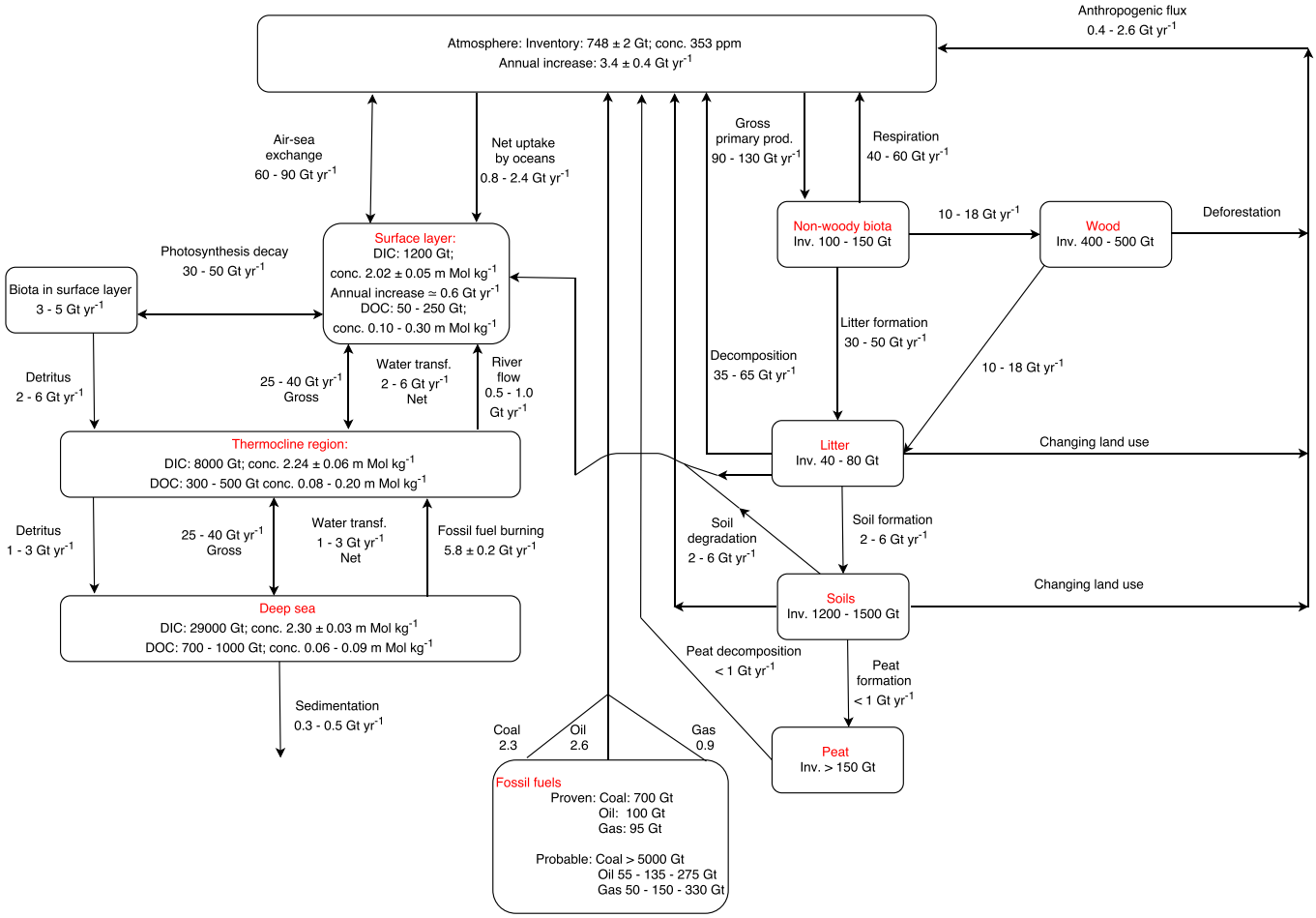

Figure 3. Diagram depicting the different compartments of the global carbon cycle and the fluxes between those. Storage is given in gigatons (10^9 tons), which is equivalent to pentagrams. Fluxes are given in gigatons per year. Modified from Bolin and Fung (1992).

fuel burning (5.6–6.0 Gt C yr^{-1}), main sources of carbon dioxide to the atmosphere include decomposition of organic residues (35–65 Gt C yr^{-1}) and plant respiration (40–60 Gt C yr^{-1}) (Bolin & Fung, 1992). Oceanic respiration is also a major source of CO_2 (55–76 Gt C yr^{-1}), and its temporal and spatial variability is discussed in del Giorgio and Duarte (2002). Currently, it is widely recognized that Earth's atmosphere is the dynamic pool containing the least amount of carbon, which, together with its homogeneity, makes it the most sensitive reservoir to perturbations in the carbon cycle (Cook et al., 2009). Oceans, in turn, hold about 50 times more dissolved inorganic carbon (DIC) than the atmosphere, with atmosphere-ocean CO_2 exchange fluxes amounting to approximately 90 Gt C yr^{-1} in each direction (see review in Falkowski et al., 2000) and, since the Industrial Revolution, a net flux of 0.8–2.4 Gt C yr^{-1} into the oceans (Bolin & Fung, 1992, and references therein). A complete discussion on carbon fluxes between reservoirs is presented by Bolin and Fung (1992).

The amount of carbon stored in a reservoir is often determined by turnover rates, as some reservoirs do not cycle carbon quickly. Carbon turnover rates for geological processes often vary from thousands to millions of years, whereas phenomena such as the plant fixation of carbon via photosynthesis involve time scales of one year or less, illustrating the concepts of *sedimentary* and *dynamic* compartments within the carbon cycle (Cook et al., 2009). In the terrestrial biosphere, carbon atoms reside on average between 4 and 8 years (Gaudinski et al., 2000) as a result of rapid exchange with the surrounding atmosphere. Exchange between the upper ocean layers and the overlying atmosphere is relatively fast, with carbon being cycled much quicker than between the surface and deep ocean. Carbon atoms can stay in the deep ocean for thousands of years (e.g., Sigman & Boyle, 2000) before returning to the atmospheric reservoir through upwelling and subsequent exchange in the ocean surface. This has the effect of establishing a dependence of marine residence

times on the water column depth. Deep ocean residence times also vary with ocean geography and circulation, whereas the surface residence times depend on the deep ocean regime and the air-sea gas exchange (Russell, 2011).

4. The Atmosphere-Ocean Carbon Cycle

The carbon cycle in the oceans is distinct from the atmospheric one, and the atmosphere-ocean gas exchange links these two reservoirs. This exchange is primarily driven by differences in partial pressures of CO_2 and is written as follows:

$$F = k_g(pCO_{2,a} - pCO_{2,s}) = k_g \Delta pCO_2 \quad (6)$$

where $pCO_{2,s}$ is the equilibrium partial pressure of CO_2 in the surface waters, $pCO_{2,a}$ is the equilibrium partial pressure in the overlying atmosphere, and k_g is a gas exchange coefficient dependent on factors such as wave agitation (wind speed) (Merlivat & Memery, 1983; Siegenthaler & Sarmiento, 1993; Takahashi et al., 2002, 2009). Molecules of CO_2 exchange across the air-sea interface and the flux is proportional to the difference in pCO_2 between the reservoirs. The atmospheric partial pressure $pCO_{2,a}$ is relatively homogeneous, and variations in the sign of the flux are determined by local $pCO_{2,s}$ (Williams & Follows, 2011), which is influenced by the interaction of deep waters with the mixed layer (Sigman & Boyle, 2000). A good example of how the CO_2 content of surface waters controls the air-sea exchange was described by Le Quéré et al. (2007), who observed that the Southern Ocean CO_2 sink has weakened despite the large increase in atmospheric CO_2. For a more detailed discussion on the effects of anthropogenic climate changes on CO_2 sinks, the reader is referred to Le Quéré et al. (2009). The air-sea gas exchange is not a uniform process over the global oceans and regions of CO_2 uptake, that is, where primary productivity occurs in areas with a permanent thermocline, and CO_2 outgassing, that is, where upwelling dominates, coexist. Globally, the integrated flux in both directions approximately cancel each other (Sigman & Boyle, 2000; Williams & Follows, 2011).

Temperature affects the solubility of CO_2 in sea water, ultimately influencing the air-sea gas exchange. Carbon dioxide is more soluble in cold and saline waters and thermohaline circulation together with ocean ventilation drive the mechanism of solubility pump (see, e.g., Raven & Falkowski, 1999; Taylor, 1992). Therefore, CO_2 sequestration is latitudinally dependent with enhanced oceanic uptake of CO_2 in cold waters at high latitudes. In these regions, the process of primary production removing CO_2 from the surface ocean, through photosynthesis followed by the death and sinking of phytoplankton (known as the ocean's biological pump), contributes to the invasion of CO_2 into the water (see, e.g., Herndl & Reinthaler, 2013; McElroy, 1983; Sarmiento et al., 1998; Siegenthaler & Sarmiento, 1993; Sigman & Boyle, 2000). Post et al. (1990) point out that an approximate equilibrium in CO_2 concentration between surface waters and atmosphere is attained relatively quickly and little CO_2 can be incorporated into the ocean without processes such as the biological pump transferring carbon to the deep ocean and thus decreasing $pCO_{2,s}$. This mechanism sequesters enough CO_2 to maintain atmospheric CO_2 concentrations 150–200 ppmv lower than they would be without phytoplankton assistance. Nearly 25% of the carbon fixed in the ocean upper layer is transported to the basin interior, with the biological pump presently accounting for the export of 11–16 Gt of organic carbon per year (Falkowski et al., 2000, and references therein). In tropical zones, warming reduces the solubility and drives oceanic CO_2 evasion (Williams & Follows, 2011). Ocean CO_2 uptake in tropical regions can be intensified by upwelling of nutrient-rich waters leading to enhanced primary production and biological pump or, conversely, upwelling can bring carbon-rich waters to the surface, increasing $pCO_{2,s}$ and leading to outgassing (Williams & Follows, 2011). Nevertheless, air-sea CO_2 fluxes in coastal upwelling systems are not straightforward (see, e.g., Hales et al., 2005; Friederich et al., 2008, and references therein). Takahashi et al. (2002, 2009) present detailed discussions on the global sea-air CO_2 flux, and a more complex control on $pCO_{2,s}$, driven by ocean chemical composition, is discussed in Sigman and Boyle (2000).

Once CO_2 dissolves in the water, it dissociates and reacts with water to form three carbonate species (carbonic acid, bicarbonate, and carbonate) collectively known as DIC, constituting the pool of inorganic carbon in the oceans (Mills & Urey, 1940; Mook et al., 1974; Siegenthaler & Sarmiento, 1993; Zeebe & Wolf-Gladrow, 2001):

$$DIC = CO_2^* + HCO_3^- + CO_3^{2-} \quad (7)$$

where CO_2^* is the sum of the aqueous form of carbon dioxide ($CO_{2(aq)}$) and carbonic acid (H_2CO_3). The amount of carbon held as DIC in the ocean is 40 times as much as that of organic forms of carbon and 90% of DIC

is made up of bicarbonate ions (Williams & Follows, 2011). Due to the biological and solubility pumps sequestrating carbon to the ocean interior, DIC concentrations increase below the thermocline, where the sinking organic carbon is oxidized by the respiration of heterotrophic organisms and converted to DIC (Falkowski et al., 2000, and references therein). Species that form $CaCO_3$ shells reduce surface DIC concentration by delivering this carbonate to the deep ocean since, upon death, these organism's shells sink to the ocean floor, where dissolution can occur. This process, called the carbonate pump, has a competing effect on $pCO_{2,s}$ (see, e.g., Volk & Hoffert, 1985). The marine carbon cycle and the factors affecting DIC in the oceans are discussed in Zeebe and Wolf-Gladrow (2001) and Williams and Follows (2011). Sarmiento et al. (1998), Joos (1999), and Falkowski et al. (2000) discuss the response of the ocean carbon reservoir to the ongoing climate change.

5. Anomalies in the Biogeochemistry of Carbon

Although not fully understood initially, inconsistent ^{14}C activities in marine samples have been reported since the very beginning of radiocarbon research. Nier and Gulbransen (1939) performed the first systematic investigation on the relative occurrence of carbon isotopes in natural sources. Based on measurements of the ratio $^{12}C/^{13}C$, they concluded that the incorporation of the heavy isotope seemed to be favored in carbonates, which were found to be enriched in ^{13}C by approximately 2.5% when compared to terrestrial material. Considering that the discrimination is due to the mass difference between the isotopes, it follows from their results that marine carbonates must be enriched in ^{14}C by as much as 5% relative to terrestrial material. This idea was supported by ^{14}C activities reported for marine carbonates in the first radiocarbon assay (Libby et al., 1949). Nevertheless, the assay highlights that the error in the measurements was large enough to overlap the predicted values for enrichment. Soon thereafter, three modern sea shells exhibited radiocarbon activities higher by nearly 8% on average than those measured for wood and other organic materials (Anderson & Libby, 1951). However, arguing that the accuracy of the fractionation factor estimation was better than the precision of their shells measurements, the authors corrected their values for carbonate using the values for modern wood and the predicted enrichment. At this point, there seemed to be a consensus on the higher ^{14}C concentration of marine carbonates relative to terrestrial material, with radiocarbon ages for these two kinds of samples presenting good agreement after isotopic fractionation corrections.

The scenario started to change when Peruvian archeological shells measured by Kulp et al. (1952) yielded ages considered to be too old. Acknowledging that shells from other upwelling localities showed the same anomaly, the influence of deep ocean waters was suggested as a cause of the effect. However, this hypothesis was discarded by Blau et al. (1953) because the radiocarbon content of five shells from locations presenting different oceanographic features (e.g., Florida, Texas, and California) were in agreement with terrestrial material. The biogeochemistry of carbonate formation was poorly understood at that time. As highlighted by Blau et al. (1953), the practice of assuming that shell ^{14}C values are higher than those of wood was in need of modification. Craig (1954) argued that the enrichment was difficult to estimate because of the large errors involved and concluded that methods with better precision did not show the radiocarbon enrichment predicted. His results showed that shell carbonate is in equilibrium with ocean water and anomalously low ^{14}C enrichment can only be explained by an oceanic radiocarbon depletion that does not affect plants. Craig (1954) tried to explain this phenomenon on the basis of biogeochemical differences between ocean and atmosphere. Considering the observed depletion of 5% in sea shells expected activity and noticing that it corresponds to an age of 400 years for surface ocean carbonates, he concluded that this effect was a product of the slow transfer of ^{14}C across the air-sea interface. Furthermore, he acknowledged that the effect should be greater in the deep ocean due to even slower mixing rates.

6. MRE: A Proper Definition

The radiocarbon community has come to recognize that, when ^{14}C dated, samples formed in environments not directly supported by atmospheric CO_2 are susceptible to yield anomalies up to several thousands years from their real age. The ^{14}C age obtained for samples from these environments is termed the *apparent age* of the sample (Mangerud, 1972). There has been a number of investigations on the source of this anomaly (e.g., Craig, 1957 on the distribution and exchange of radiocarbon among different reservoirs) and others aiming to evaluate the reliability of radiocarbon ages obtained from marine samples (e.g., Berger et al., 1966; Taylor & Berger, 1967). These studies consider the association between apparent ages and ocean dynamics,

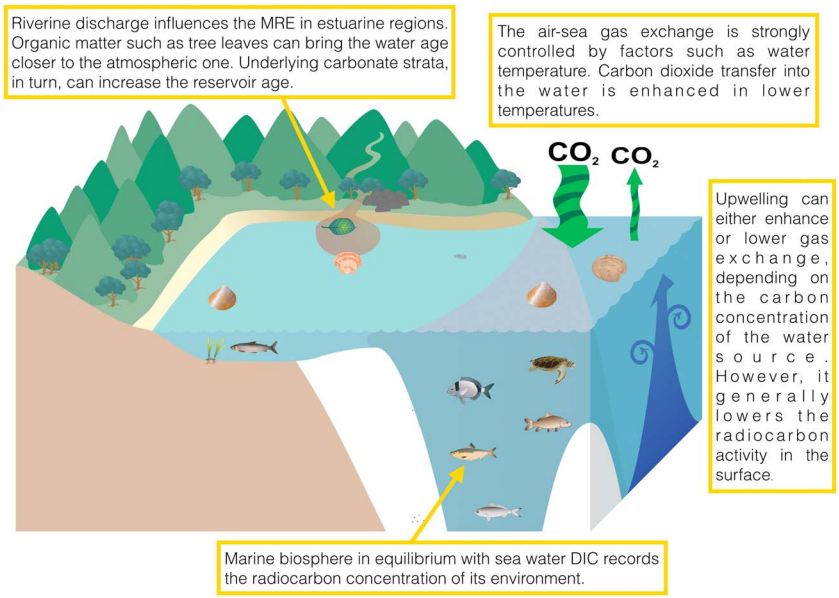

Figure 4. Summary of some of the mechanisms impacting the radiocarbon MRE in a coastal region. Some graphic elements are courtesy of the Integration and Application Network, University of Maryland Center for Environmental Science (http://ian.umces.edu/symbols/).

especially in upwelling areas. However, for the first complete analysis of this topic, the reader is referred to Mangerud (1972), who addressed common problems involved in shell ^{14}C ages and concluded that when handled carefully, shell dates are reliable.

Regarding ^{14}C interreservoir transport, Mangerud (1972) points out that no equilibrium is reached between atmosphere and oceans, with a steady state situation occurring. The air-sea gas exchange alongside slow internal oceanic mixing leads to comparatively low radiocarbon activity in the oceans versus the atmosphere, which in turn causes apparent ages in marine carbon. Bard (1988) presents an equation for the determination of the $^{14}C/^{12}C$ ratio of surface waters depending on several climate-related parameters and discusses, for instance, the effect of wind speed on the MRE. The oceanic reservoir of DIC is about 50 times larger than the atmospheric one with much longer residence times in the deep ocean (in the order of 1,000 years compared to 5 years in the atmosphere) (Levin & Hesshaimer, 2000; Sigman & Boyle, 2000), and the dominant factor controlling ocean ^{14}C activity is ocean circulation (Mangerud, 1972). This is because CO_2 is transferred only at the air-sea interface, and water masses removed from this boundary undergo radioactive decay, presenting lower radiocarbon activity depending on how long the water has been at depth. As surface water contains a mix of old carbon from the deep ocean and new carbon from the atmosphere, its radiocarbon activity is enriched relative to isolated deep waters but depleted when compared to the atmosphere and terrestrial biosphere (Ascough et al., 2004). These processes removing ^{14}C from a reservoir (or equivalently introducing preaged carbon) without the presence of a counter process replenishing it cause a *reservoir effect*. The processes discussed above and summarized in Figure 4 cause a difference in levels of radiocarbon depletion among distinct marine environments (Gordon & Harkness, 1992), showing the inherent geographical variability of the MRE.

After understanding the presence of reservoir effects, the next step was to standardize the way in which radiocarbon laboratories report marine ages. Stuiver and Polach (1977), in a seminal paper on radiocarbon dating, defined the term *reservoir effect* for the first time and made recommendations on how to deal with it. Nevertheless, a formal mathematical definition for the terms involved in the offset in radiocarbon activity between ocean and atmosphere was still lacking.

A full discussion on the calibration of marine radiocarbon ages, including a mathematical definition for the MRE, was first presented by Stuiver et al. (1986), who introduced the concept of reservoir age $R(t)$ as being the difference between the radiocarbon age of a marine sample and its atmospheric age determined independently for a given time t:

$$R(t) = {}^{14}C_{\text{marine}} - {}^{14}C_{\text{atmospheric}} \quad (8)$$

As their model was not able to accommodate local effects, the authors introduced the concept of ΔR as a way of accounting for oceanic mixing processes that contribute to the MRE. The ocean is composed of very heterogeneous water masses that occasionally mix (see Broecker, 1991; Talley, 2013; Talley et al., 2011, for a discussion on the global scale overturning circulation) and due to the great variety and complexity of mechanisms involved in the MRE, it is unreasonable to apply a global correction to marine ages. Cook et al. (2009) state that due to slow mixing rates, particularly of deep waters, the ocean is the most heterogeneous reservoir in terms of its ^{14}C distribution. The term ΔR is defined as the difference between the regional and the modeled global marine reservoir ages, where the latter is the offset between the atmospheric and marine calibration curves for any point in time from the present back through the curve (see section 2, Stuiver et al., 1986, and Stuiver & Braziunas, 1993):

$$\Delta R = R_{\text{measured}} - R_{\text{expected}} \tag{9}$$

In Stuiver et al. (1986), equation (9) is written as follows:

$$\Delta R = P - Q \tag{10}$$

where P is the radiocarbon age measured for a marine sample and Q is the modeled global marine age obtained from the radiocarbon age of the coeval atmosphere. Equation (10) can easily be obtained using equation (8) and changing notation. Consistent with the definition given in Stuiver et al. (1986), ΔR values were initially assumed to be time independent in first approximation. Nevertheless, there has been evidence strongly supporting the opposite (e.g., Austin et al., 1995; Kennett et al., 1997; Ortlieb et al., 2011; Soares & Dias, 2006).

Stuiver et al. (1986) derived a smooth marine calibration curve, reflecting the strong attenuation in the oceans of the high-frequency atmospheric $\Delta^{14}C$ perturbations, going back to 7,000 BC. The first ΔR values, calculated from previously published marine dates, are also given in their study. Soon thereafter, Stuiver and Braziunas (1993) improved and extended the atmospheric record for the modeled surface layer of the global ocean to 10,000 BC.

Reservoir offsets for estuaries, lakes, and peatlands must be treated on an individual basis. Freshwater and hardwater effects altering the radiocarbon signal of estuaries are not MREs per se. Riverine discharge can introduce exogenous carbon to the marine environment and significantly impact the MRE in estuaries. Freshwater reservoirs are usually shallower than the ocean and often less or not stratified, which enhances CO_2 exchange with the atmosphere and, consequently, increases the input of recently formed carbon species, decreasing ΔR. Additionally, the breakdown of organic detritus (e.g., tree leaves) carrying a terrestrial radiocarbon signal can lower ΔR values, whereas rivers running on carbonate strata can carry dissolved old carbon and increase ΔR values. The mineralization of ancient dissolved organic carbon (DOC) (e.g., derived from peats), is likely to increase the radiocarbon ages of DIC in freshwater systems (Olsson, 1983, 1996), leading to elevated ΔR values. In theory, the same would happen in marine systems, but experimental data showing significant DOC influence are lacking. Discussions on these topics are available in Godwin (1951), Deevey et al. (1954), Little (1993), Heier-Nielsen et al. (1995), Ulm (2002), and Olsen et al. (2017).

7. Methodological Approaches to Assessing the MRE

The depleted ^{14}C activity of the marine reservoir relative to the atmosphere can be quantified by a variety of methods. For calibration reasons, MRE studies usually involve the determination of ΔR values much more often than $R(t)$.

One needs both marine and atmospheric ^{14}C activity—or equivalently ^{14}C concentration—at a given time in order to derive a ΔR value. The radiocarbon dating of a marine organism in equilibrium with the ambient seawater is straightforward in providing the marine ^{14}C activity for the studied region, but it is also necessary to obtain the ^{14}C activity of the coeval atmosphere. Therefore, there is a set of methods with different degrees of reliability and potential to yield the corrections. The two most common approaches to quantifying MREs make use of the following:

Known-age marine material. Essentially, any marine sample for which the organism death date is known has the potential of yielding a ΔR value. These samples were ideally collected before 1950 AD to avoid the bomb ^{14}C signal and thus are referred to as prebomb samples. They can be found deposited in museum

collections, and O'Connor et al. (2010) list and define the criteria to be followed for their selection. Phenomena such as earthquakes can expose marine organisms, acting as a temporal marker for the death date of the animals and therefore creating known-age natural deposits (see Shishikura et al., 2007). The known-age samples approach has mostly been performed using marine sedentary mollusk shells (e.g., Bowman, 1985; Bowman & Harvey, 1983; Berkman & Forman, 1996; Forman & Polyak, 1997; Hadden & Cherkinsky, 2015; Hjort, 1973; Ingram & Southon, 1996; Kuzmin et al., 2007; Mangerud & Gulliksen, 1975; Petchey et al., 2004, 2008; Siani et al., 2000; Sikes et al., 2000; Yoneda et al., 2000) although it has been shown that radiocarbon intrashell variability may be a significant source of error (see Culleton et al., 2006; Jones et al., 2007). Corals (see, e.g., Bolton et al., 2016; Druffel & Griffin, 1999), fish otoliths (see, e.g., Higham & Hogg, 1995), fish bones (see, e.g., Petchey & Clark, 2010), and even marine mammal bones (see, e.g., Olsson, 1980) have also been used in this approach.

Paired marine/terrestrial samples. For the case in which the organism death date is unknown, one can radiocarbon date a contemporaneous terrestrial sample to obtain the ^{14}C activity of the coeval atmosphere. These so-called paired marine and terrestrial samples are commonly recovered from the archeological context but can also be found buried in coastal sediments (see Kovanen & Easterbrook, 2002; Southon et al., 1990). In any case, samples must be selected with extreme care in order to assure contemporaneity (see Ascough, Cook, & Dugmore, 2005, for the major factors for consideration when using this approach). There are a number of MRE studies that have employed the paired sample methodology to determine ΔR corrections (e.g., Albero et al., 1986; Dettman et al., 2015; Facorellis, 1998; Hadden & Cherkinsky, 2017; Head et al., 2016; Latorre et al., 2017; Nakamura, 2007; Owen, 2002; Southon et al., 1995; Southon & Fedje, 2003). The atmospheric counterpart of marine samples in these studies is generally charcoal, but recent work has been done employing land snail shells (see Macario, Alves, Chanca, et al., 2016)—it has been shown that some species are reliable proxies for the atmospheric carbon reservoir (see Macario, Alves, Carvalho et al., 2016)—and terrestrial mammal bones (see, e.g., Ascough, Cook, Church, et al., 2007; Ascough, Cook, Dugmore, & Scott, 2007) for that purpose.

The use of an alternative dating method (e.g., U/Th dating) to obtain the marine sample age free of ^{14}C reservoir effects (e.g., Clark et al., 2016; Druffel et al., 2008; Edwards et al., 1993; Hall et al., 2010; Hua et al., 2015; Komugabe et al., 2014; McGregor et al., 2008; Weisler et al., 2009) or the use of volcanic ash as stratigraphic marks (for a discussion on tephrochronology see, e.g., Lowe, 2011; Sarna-Wojcicki, 2000) to link terrestrial and marine records, obtaining coeval samples for MRE studies (e.g., Austin et al., 1995; Bard et al., 1994; Eiríksson et al., 2004; Siani et al., 2013; Sikes & Guilderson, 2016; Sikes et al., 2016, 2000), have also been applied to determine both deep and surface reservoir ages. It has also been shown that, in some locations, other geochemical parameters can be a proxy for MRE offsets (e.g., Lougheed et al., 2016).

Naturally, each method has its own advantages and disadvantages. These are discussed in Ascough, Cook, and Dugmore (2005), who also address the use of tephra onshore/offshore isochrons for MRE determination and the suitability of marine and terrestrial material (see McFadgen, 1982 for a discussion on the old-wood effect). Ascough, Cook, Dugmore, Scott, and Freeman (2005) provide a discussion of possible confounding factors in shell radiocarbon measurement such as species-dependent feeding habits and habitats (see, e.g., Dye, 1994; Forman & Polyak, 1997; Hogg et al., 1998; Petchey et al., 2012). Russell, Cook, Ascough, Barrett, and Dugmore (2011) compare results obtained from a mollusk and a fish species.

There is no consensus about the best approach to calculate ΔR corrections. The first method (known-age samples) is temporally limited, although continuous ΔR records can be achieved through the analysis of annually resolved growth lines (for a discussion on schlerochronology see, e.g., Hudson et al., 1976; Gröcke & Gillikin, 2008; Marchitto et al., 2000; Oschmann, 2009) in shells (see, e.g., Butler et al., 2009) for example. The second approach (paired samples) relies on guaranteeing the contemporaneity of the pairs. The choice of method would depend on the MRE research objectives, taking into account advantages and limitations of each approach (see Table 2 in Ascough, Cook, & Dugmore, 2005).

The steps to be taken for ΔR calculation vary according to the method adopted (see equation (9) and Figure 5). Following the known-age approach, the collecting (death) year of the sample is interpolated to a marine calibration curve to generate a marine ^{14}C age. This modeled age is the second term of equation (10) and is subtracted from the measured age in order to yield a ΔR value. In the paired sample approach, Q is generated by the conversion of the terrestrial ^{14}C age via interpolation of an atmospheric calibration curve with a marine calibration curve (see Figure 1 in Russell, Cook, Ascough, Scott et al., 2011) or taking into account

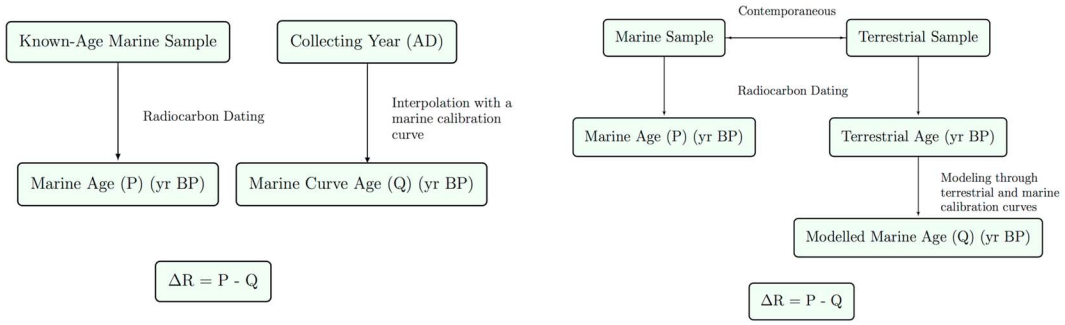

Figure 5. Diagrams illustrating the steps to be taken toward the determination of ΔR offsets using the known-age and paired methods.

probability density functions generated by the calibration (with a atmospheric curve) and reverse-calibration (with a marine curve) of the terrestrial ^{14}C age (see figures in Reimer & Reimer, 2016). The errors involved in individual ΔR estimates are also calculated differently depending on the approach used. For the known-age sample approach, Reimer and Reimer (2016) state that the ΔR uncertainty is the uncertainty of the marine ^{14}C measurement. For the paired approach, this uncertainty is given by the following propagation of errors:

$$\sigma_{\Delta R} = \sqrt{\sigma_w^2 + \sigma_m^2} \tag{11}$$

where σ_w is the error on the measured marine age and σ_m is the error on the modeled marine age. Alternatively, Reimer and Reimer (2016) propose the use of a convolution integral to obtain a confidence interval for a ΔR value derived from the paired-samples approach. Ascough et al. (2017), using the paired approach, compared the Russell, Cook, Ascough, Scott, and Dugmore (2011) and Reimer and Reimer (2016) methods for the calculation of ΔR values and found the results to be indistinguishable. The larger confidence intervals derived from the latter make it the more conservative one. Similarly to radiocarbon ages (see Ward & Wilson, 1978), the pooled mean is used for combining ΔR values:

$$\mu = \frac{\sum_i \frac{\Delta R_i}{\sigma_i^2}}{\sum_i \frac{1}{\sigma_i^2}} \tag{12}$$

where μ is the weighted mean of ΔR and σ_i is the uncertainty in ΔR_i. Whenever averaging ΔR values, Stuiver et al. (1986) recommend standard deviations based on the unweighted scatter of the data:

$$\sigma_{\text{mean}} = \frac{\sigma_u}{\sqrt{n}} \tag{13}$$

where n is the number of values and σ_u is the unweighted standard deviation of the set of ΔR values, or measurement precision:

$$\sigma_\mu = \sqrt{\frac{1}{\sum_i \frac{1}{\sigma_i^2}}} \tag{14}$$

whichever is larger. The Marine Reservoir Database (Reimer & Reimer, 2001) adopts a similar approach and the weighted error:

$$\sigma_w = \sqrt{\frac{\frac{1}{n-1}\sum_i \left(\frac{\Delta R_i - \mu}{\sigma_i}\right)^2}{\frac{1}{n}\sum_i \frac{1}{\sigma_i^2}}} \tag{15}$$

is compared to equation (14). The larger of the two is reported as the uncertainty of the averaged ΔR.

In order to ensure sample contemporaneity in the paired approach and arguing that a single pair would not represent the overall variability in ΔR, Russell, Cook, Ascough, Scott, and Dugmore (2011) propose the use of a multipair methodology in which several entities from each reservoir are selected for the ΔR calculation

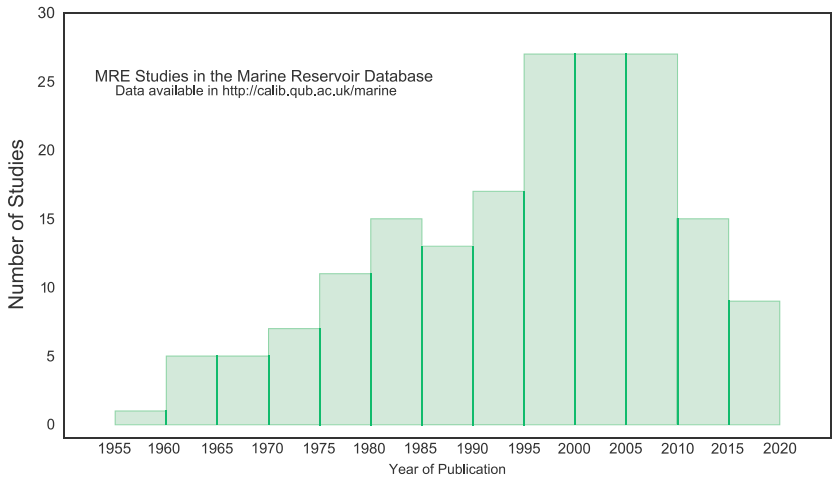

Figure 6. The histogram shows the temporal distribution of MRE studies using the known-age approach to calculate ΔR corrections. Data available at http://calib.qub.ac.uk/marine.

and every possible pairing is used. This procedure allows assessment of the security of the archeological context through the chi-square (χ^2) testing of ^{14}C ages, with a critical value varying according to the number of measurements in each group. Whenever the T statistics is less than the critical value for the number of samples in a group, samples within this group are considered to be coeval (see Ward & Wilson, 1978). Russell, Cook, Ascough, Scott, and Dugmore (2011) also make recommendations on how to report ΔR values from the multipair approach to show the inherent variability in ΔR calculations. Additionally, they showed that results of the chi-square test using two different sets of data argue against the common practice of rounding ^{14}C ages and associated errors. Moreover, the authors discuss sources of uncertainty in ΔR determinations, advocating that when calculating weighted average ΔR values, the associated errors should encompass both the standard deviation of the distribution and error on the mean:

$$\sigma = \sqrt{\sigma_{\mu}^2 + \sigma_{w}^2} \tag{16}$$

A number of studies have used the multipair approach (e.g., Edinborough et al., 2016; Martins, 2013; Macario et al., 2015; Monge Soares et al., 2016). More recently, Macario et al. (2015) introduced the use of a calibration program for ΔR determinations. Following the code in Bronk Ramsey and Lee (2013), the authors employed the OxCal v4.2.3 platform (Bronk Ramsey, 2009) to generate a probability distribution for a ΔR value derived from marine and terrestrial samples from an archeological shellmound. This method has proved to yield results statistically equivalent to the multipair approach and has been repeated in studies involving the known-age (e.g., Faivre et al., 2015) and paired (e.g., Zazzo et al., 2016) approaches. Translating a calibrated age range into the ^{14}C time scale prior to the calculation of reservoir age offsets (R values) (an uncalibration-convolution process) is the approach proposed by Soulet (2015), who argues that this method would fully account for uncertainties bounded to the radiocarbon age of the sample, the independent calendar age, and the calibration curve itself. The author presents open-source codes for the two main approaches discussed here as well as for the case in which there is a degree of uncertainty in the calendar age of the sample. Subsequently, noting that conventions such as those established for reporting radiocarbon ages were lacking for the report of ^{14}C age offsets, Soulet et al. (2016) discussed a common framework for the latter, encouraging the adoption of this framework within the radiocarbon community.

8. The Marine Reservoir Database

The importance of the MRE is now widely recognized and the need for ΔR values led the scientific community to empirically calculate such corrections. In recent years, this significantly increased the number of ΔR values available for locations worldwide (Figure 6). Nonetheless, publications compiling these values are impractical because new data are constantly being produced. A dynamic tool allowing the user to explore ΔR values over the globe for archeologists, oceanographers, and other researchers working with radiocarbon in the marine environment was developed by Reimer and Reimer (2001). This online platform,

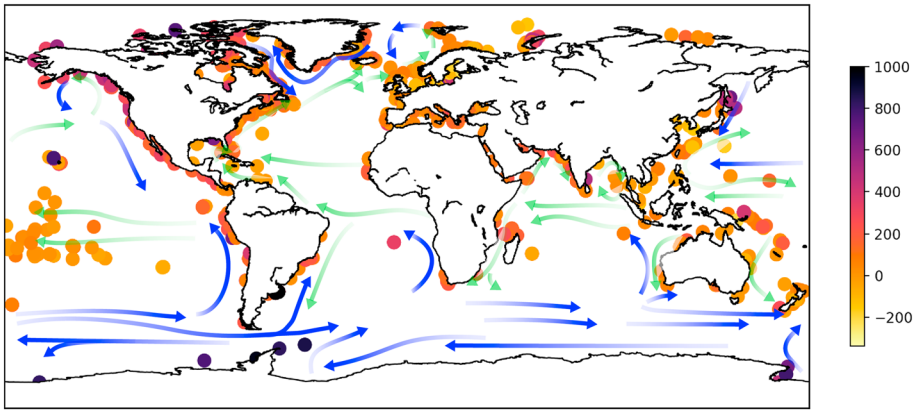

Figure 7. ΔR values (in ^{14}C yr) plotted in a color scale alongside with warm (green) and cold (blue) ocean currents. Upwelling zones, such as the west coast of the United States constitute ocean areas with especially distinct MRE characteristics. Data from The Marine Reservoir Database, which also holds the references for each value.

called The Marine Reservoir Database, holds ΔR values for the modern surface ocean alongside with their references (http://calib.qub.ac.uk/marine/). The interface to the database shows a world map in which the user chooses their research region to obtain the relevant information. Whenever a reservoir correction value is used in a publication, the respective reference must be cited. Figure 7 shows all ΔR values available on the database up to the present date. Despite the high variability in the data, most of the values are between −100 and +100 ^{14}C yr and it is possible to see a correlation between the magnitude of values and major ocean circulation. Although the great majority of ΔR values are derived from coastal regions, where the influence of other factors can dominate, it is possible to see that the largest ΔR values are in the Southern Ocean followed by zones of coastal upwelling in the Pacific. Notably, the Southern Ocean is ^{14}C depleted due to the upwelling of old deep water and the melting of ice, changing water properties (see, e.g., Berkman & Forman, 1996; Hall et al., 2010; Sikes & Guilderson, 2016; Sikes et al., 2008, and references therein). The upwelling that affects the west coasts of the United States and South America (see, e.g., Huyer, 1983; Strub et al., 1998, respectively), for example, is also documented by the darker points in these regions of the map. On the other hand, in the Baltic Sea, for example, Lougheed et al. (2013) found low ΔR values and correlated them with terrestrial runoff, showing a robust relationship between $R(t)$ and salinity.

The database also provides ^{14}C ages and the R' values defined in section 9. The collection of data described here is composed exclusively of known-age marine samples from depths shallower than 75 m, to ensure they represent the mixed layer, and information such as δ^{13}C values or species and feeding habits is reported depending on whether these are available in the original publication (Reimer & Reimer, 2001).

At present, the CHRONO Marine Reservoir Database contains over 450 ΔR values, which are not homogeneously distributed across 65 regions. When ΔR values are not available for specific sites, offsets from nearby locations may be used instead. Nevertheless, the user should be aware of possible errors involved when locations lie across distinct oceanographic settings, as discussed and exemplified by Hinojosa et al. (2015). In addition, the use of modern values to correct old ages can be problematic (Hua et al., 2015). Below, we explore the information provided by the database and, although the data are temporally limited to the most recent section of the calibration curves, some interesting features of the MRE can be discussed.

9. MRE in the Calibration Process

Due to the air-sea gas exchange, fluctuations in atmospheric ^{14}C activity are partially reflected in the marine environment, making it reasonable to expect that marine ages must undergo calibration similarly to terrestrial ones. However, marine calibration has more steps as the MRE prevents the use of an atmospheric calibration curve or a global marine curve. The oceanic response to fluctuations in the atmospheric radiocarbon activity, discussed in section 6, explains the smoother marine curves and justifies their use. The marine curve for the surface mixed layer developed by Stuiver and Braziunas (1993) has been continuously refined by the radiocarbon community. The most recent version of a marine calibration curve is the internationally accepted Marine13 (Reimer et al., 2013) starting from 1950 AD and going back 50,000 years. Marine13 was

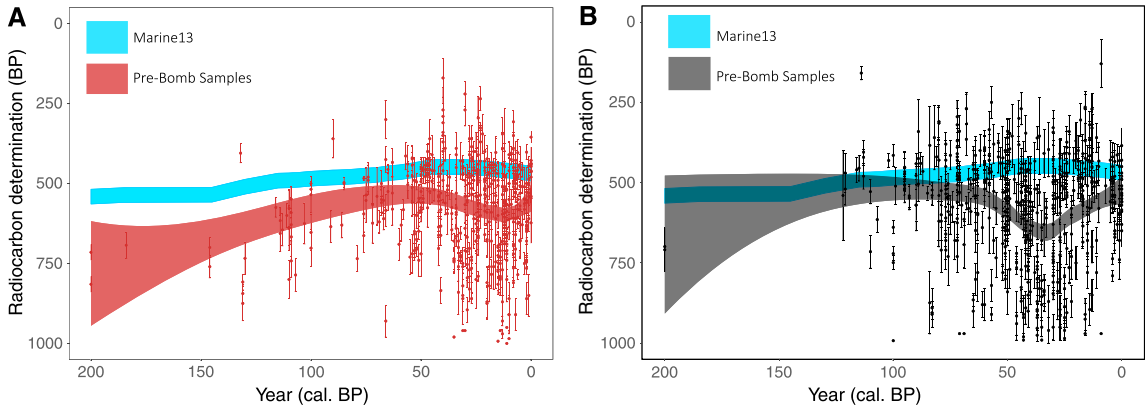

Figure 8. Deviations of marine radiocarbon ages held in the Marine Reservoir Database from (a) low and middle (between 40° N and 40° S) and (b) high (higher than 40°) latitudes from the most recent section of Marine13.

constructed based on tropical and subtropical records, and Reimer et al. (2013) state that care must be taken when calibrating ages from higher latitudes. However, Figure 8 shows that there are significant deviations of the Marine Reservoir Database prebomb radiocarbon ages from the most recent section of Marine13 for both zones. This reinforces the spatial variability of the MRE (due to factors discussed in section 6) and illustrates that samples from different regions inside tropical and subtropical zones are subjected to variable oceanic radiocarbon deficiency. If this is not accounted for in the calibration of radiocarbon ages from these geographical regions, important oceanic features such as the upwelling that takes place on the Peruvian coast (see, e.g., Strub et al., 1998) would be neglected. Due to the strong spatial dependence of the MRE, a global curve cannot fully account for regional effects and the ideal approach would be the construction of regional calibration curves. Without this, the use of ΔR values to bring the measured radiocarbon ages to a global context remains the best option. The lack of continuous highly resolved records, equivalent to tree rings, in the marine environment (Stuiver & Braziunas, 1993), turns the robust reconstruction of oceanic ^{14}C fluctuations into a complex task and hinders the construction of regional marine calibration curves, although some attempts have been made (see, e.g., Bondevik et al., 2006; Deo et al., 2004). Despite making use of archives such as fossil corals, sections of Marine13 had to be based on the application of numerical models to simulate the oceanic response to atmospheric variations in ^{14}C content (Reimer et al., 2013). The high spatial and temporal variability of the MRE would require the radiocarbon dating of a great number of samples from the same region to achieve a reliable regional curve, possibly demanding efforts from different research groups working on the same geographical area. Alternatively, approaches based on MRE models such as the one described in Butzin et al. (2017) or the development of a Bayesian offset model for ΔR (Reimer & Reimer, 2006) would also be possible. The construction of regional marine calibration curves may be an especially interesting approach for very particular regions lacking reliable sediment archive chronologies and where reservoir ages are thought to have varied greatly over time (Soulet, 2015, and references therein).

Calibration is a concern especially in fields such as archeology. Certainly, the MRE imposes obstacles for accurate calibration of dates obtained from marine-derived carbon samples. Indeed, human populations have been heavily exploiting marine resources for millenia, leaving records of their habits through deposition of marine material in archeological sites near shorelines (see Erlandson et al., 2008, and references therein). Fortunately, the MRE issue can be dealt with using specific corrections incorporated in the calibration process.

The terms involved in the MRE and explained in section 6 are represented in Figure 9. Global R or R_g is the highly time-dependent difference in radiocarbon age between the atmosphere and the global ocean, reflecting changes in the atmospheric ^{14}C concentration. Graphically, R_g is the difference between the atmospheric and marine curves at any point. ΔR, being the offset in ^{14}C activity between the local and the global oceans, must be subtracted from the measured radiocarbon age of the sample before it can be calibrated with a global curve such as Marine13. Graphically, ΔR would appear as the difference between a measured marine radiocarbon age and the marine curve at a given calendar year. Finally, $R'(t)$ is defined as the difference in radiocarbon age between the local ocean and its overlying atmosphere. In Figure 9, it appears as the difference between the atmospheric curve and the measured marine radiocarbon age for a given calendar year.

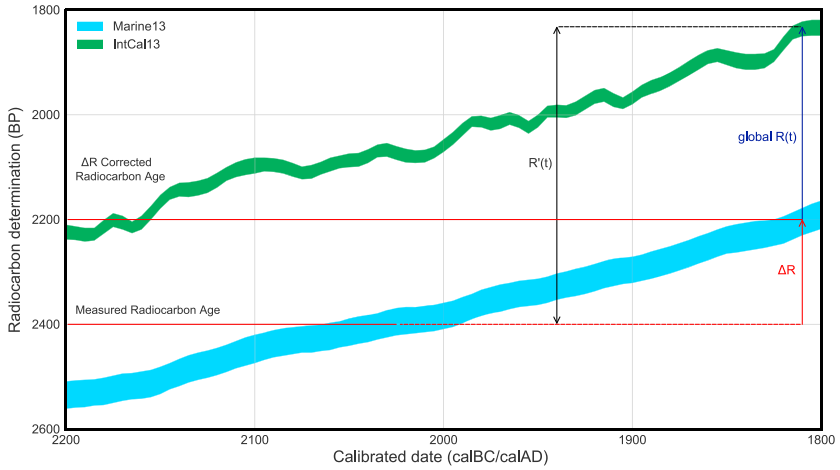

Figure 9. Graphical representation of the terms involved in the MRE as firstly defined by Stuiver et al. (1986). The green and blue curves represent sections of IntCal13 and Marine13, respectively. Data from Reimer et al. (2013).

The value of $R'(t)$ can be used to correct marine ages prior to calibration. The procedure would be subtracting R from the measured marine age and then calibrating the result with an atmospheric calibration curve such as IntCal13 or SHCal13 (Hogg et al., 2013). Stuiver and Braziunas (1993) present this possibility but advocates against it, noting that although atmospheric and marine curves follow the same long-term trend, short-term atmospheric fluctuations are absent in the latter. Differences between the atmospheric and marine curves explain why ΔR values are often the quantities of interest in archeological research. For shallow reservoirs, in ^{14}C equilibrium with the overlying atmosphere, the use of $R(t)$ and an atmospheric calibration curve may be the most accurate approach.

ΔR_a is the atmospheric equivalent of ΔR, accounting for regional atmospheric effects that could lead to intrareservoir discrepancies in radiocarbon activity (Stuiver & Braziunas, 1993). ΔR_a is significant for interhemispheric variation (Hogg et al., 2011, 2013; Lerman et al., 1970; McCormac et al., 1998, 2002; Stuiver, Reimer, & Braziunas, 1998; Vogel et al., 1993) and is automatically taken into account through the use of specific curves for the Northern and Southern Hemispheres.

All these terms are related by the following equation (from Stuiver & Braziunas, 1993):

$$R'(t) = \text{global } R(t) + \Delta R \tag{17}$$

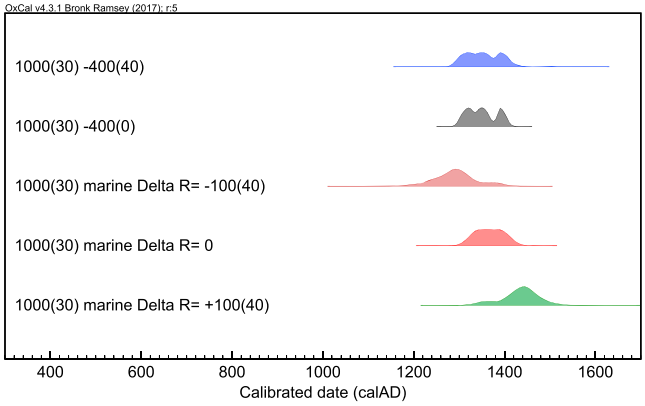

Figure 10. The effect of different MRE corrections in marine calibration for a sample with a ^{14}C age of 1,000 ± 30 ^{14}C yr BP calibrated with IntCal13 with a correction of 400 ^{14}C yr, with (blue) and without (black) an uncertainty of 40 ^{14}C yr. Then the same value is calibrated with the Marine13 curve with ΔR values of −100 ± 40 (pink), 0 (red), and +100 ± 40 ^{14}C yr (green) (after Cook et al., 2015).

The effect of the MRE correction steps toward the calibration of a marine age can be observed in Figure 10. In this example, we assume a radiocarbon age of 1,000 ± 30 ^{14}C yr BP obtained from a marine sample. For the top two probability density functions, an offset of 400 ^{14}C yr is subtracted from the age and calibration is then performed with the atmospheric curve IntCal13. This procedure is adopted with an uncertainty of 40 ^{14}C yr to account for fluctuations in the offset (blue) and with no uncertainty (black). The results display the oscillations characteristic of the atmospheric curve but unrealistic for the marine reservoir. Alternatively, the marine curve can be used directly, resulting in a smoother distribution. For the bottom three distributions, ΔR values of −100 ± 40 ^{14}C yr (pink), 0 ^{14}C yr (red), and +100 ± 40 ^{14}C yr (green) were used in order to show their influence on the calibrated age. Not only the calibrated age range is shifted to the right or to the left relative to the uncorrected calibration but it can get closer or farther from plateaus in the calibration curve. As noted by Cook et al. (2015), the use of a ΔR correction and its uncertainty is likely to cause a loss in precision but the probability distribution for the calibrated age will be a more accurate reflection of the true age.

The calibration of partially marine samples is more complicated than that of wholly marine samples since although we can assume that carbon in oceanic

organisms far from estuaries is of complete marine origin, the same is not true for mixed diet organisms (e.g., humans). In this case, stable isotope analyses (of carbon, nitrogen and/or sulfur) provide an estimation of the percentage marine diet and establish to which extent the sample is marine (Bayesian mixing models such as the Food Reconstruction Using Isotopic Transferred Signals (FRUITS) can be used for this purpose (see Fernandes et al., 2014)) and a mixed calibration curve is applied (see, e.g., Arneborg et al., 1999; Beavan & Sparks, 1998; Beavan-Athfield et al., 2001; Commendador, 2014; Cook et al., 2015; Ervynck, 2014; Naito et al., 2010 for details).

10. Applications of the MRE

The MRE finds application in a wide variety of fields, reflecting the influence of the oceanic carbon cycle and its control on many aspects of climate. As a consequence of radiocarbon dating importance in archeology, the MRE is of interest for archeological research and many of the available data were obtained by archeologists or other scientists working in archeology-related departments all over the world (e.g., Ervynck, 2014; Facorellis & Vardala-Theodorou, 2015; Little, 1993; Ulm, 2002). Nevertheless, it is the applicability of radiocarbon dating to oceanic studies that is discussed in the next paragraphs.

Concerning the ocean sciences, the problem of understanding the dynamic influence of ocean circulation upon reservoir ages is a complex one, demanding the use of various techniques. The tracer characteristics of ^{14}C have been explored in a number of oceanographic studies in which the main objective is to investigate ocean circulation modes, residence times, upwelling strength, or even how changes in ^{14}C disequilibria modulate the atmospheric radiocarbon concentration, leading to a better understanding of the ocean system and its response to climate variation (e.g., Adkins, 1998; Adkins & Boyle, 1997; Burke et al., 2015; Hines et al., 2015; Sikes & Guilderson, 2016; Sikes et al., 2000, 2016; Skinner et al., 2010, 2015). Therefore, the calculation of marine reservoir ages is essential to understanding how oceanic and continental climate relate and, as Russell, Cook, Ascough, Scott, and Dugmore (2011) point out, radiocarbon MREs have been used as proxies for changes in localized ocean regimes (e.g., Druffel & Griffin, 1993). One of the first radiocarbon studies in oceanography was conducted by Broecker et al. (1960), aiming to establish the geographic and depth distribution of ^{14}C in the North Atlantic. This was followed by many other studies (e.g., Bard, 1988; Druffel et al., 1989; Ortlieb et al., 2011; Shackleton et al., 1988; Williams et al., 1969), showing the power of this approach.

The time elapsed since the last contact between a parcel of seawater and the atmosphere is commonly referred to as the age of this water (e.g., England, 1995), and the process through which surface waters flow into the deep ocean is termed ocean ventilation (e.g., England & Maier-Reimer, 2001; Khatiwala et al., 2012). When oceans ventilate, surface waters sink into the interior of the ocean and transmit their physical and chemical signatures to deep waters. Therefore, it follows that any phenomenon interfering with the patterns and rates of ocean ventilation will strongly affect ^{14}C distribution within the ocean as demonstrated by extreme fluctuations in ocean circulation during the last deglaciation, leading to variation in air-sea exchanges and reservoir ages (see, e.g., Bard, 1988; Bard et al., 1989; Broecker & Barker, 2007; Stuiver et al., 1991). Measuring ^{14}C age offsets between surface and deep waters is an accepted method of assessing past deep ocean ventilation rates (Broecker et al., 2004). Approaches—discussed in detail by Broecker et al. (2004)—include the radiocarbon dating of coexisting planktonic and benthic foraminifera (see, e.g., Andree et al., 1986; Broecker et al., 1984; Keigwin, 2004), ^{14}C and Uranium series measurements of age-matched surface water and deep dwelling corals (e.g., Goldstein et al., 2001) and the ^{14}C dating of benthic foraminifera and terrestrial material associated with the same tephra horizon (e.g., Sikes et al., 2000).

Studies involving marine radiocarbon measurements and/or modeling have been performed in different basins, with distinct time scales and different types of samples. There have been many independent studies of oceanic paleoventilation and calculation of reservoir ages, ultimately assisting in the reconstruction of past climatic events (Andree et al., 1986; Bard, 1988; Björck et al., 2003; Bolton et al., 2016; Broecker, 1991; Broecker et al., 1988, 2004; Burr et al., 2015; Butzin et al., 2005; Carré et al., 2016; Cook & Keigwin, 2015; de la Fuente et al., 2015; Douarin et al., 2016; Druffel & Suess, 1983; Druffel et al., 1998; Hall et al., 2010; Hua et al., 2015; Hughen et al., 1998; Ikehara et al., 2011; Kennett et al., 1997; Kovanen & Easterbrook, 2002; Komugabe-Dixson et al., 2016; Marchitto et al., 2007; Ritz et al., 2008; Sarnthein et al., 2007; Shen et al., 2004; Stern & Lisiecki, 2013; Wündsch et al., 2016, to cite a few). Radiocarbon research in the ocean sciences community is widespread, and studies focusing on periods of extreme climate, when great variations in the MRE are likely to occur, are especially common. For instance, numerous studies have characterized oceanic conditions during

the Younger Dryas (YD). Not surprisingly, many of these studies have based their conclusions on the quantification of the MRE and its changes through time, showing how different factors interplay to control the effect in different oceans. The YD was a severe millennial-duration cold spell that marked the termination of the last glacial period (12.9–11.7 kyr BP) (Broecker et al., 2010). In the North Atlantic Ocean, the reduced advection of surface waters and the decrease of atmosphere-ocean CO_2 exchange because of the presence of sea ice have been linked to high reservoir ages during the YD (see, e.g., Bard et al., 1994; Bondevik et al., 2006; Stocker & Wright, 1996). In the Mediterranean Sea, YD reservoir ages similar to modern values were attributed to patterns of ocean circulation bringing young subtropical Atlantic waters (Siani et al., 2001). In the Indian Ocean, a varying relative contribution of summer monsoon upwelling, winter monsoon surface convection, and the thermocline reservoir age controlled the high and variable reservoir ages of the Arabian Sea surface during the YD (Staubwasser et al., 2002). The list of studies of the paleo-MRE is long and, moving on to other geographical regions, recent references for the Pacific Ocean basin can be found in studies such as Lindsay et al. (2015), Sikes and Guilderson (2016), and Sikes et al. (2016). Finally, although not focusing on the MRE, reviews such as Archer et al. (2000) and Past Interglacials Working Group of PAGES (2016) discuss key concepts involved in Glacials/Interglacials cycles, presenting valuable information on the global carbon cycle and assessing mechanisms involved in the control of atmospheric and oceanic CO_2, which ultimately relate to the MRE.

Marine data sets corrected for MRE are essential for the construction of both marine and atmospheric calibration curves (see details of the construction procedures of the last calibration curves in Hogg et al., 2013, Reimer et al., 2013) and the few examples mentioned above give an idea of the importance of radiocarbon oceanic research, the multidisciplinary character of the method and its power to approach present world relevant questions such as the Earth's climate system.

The relatively high signal of bomb-produced radiocarbon in the upper oceanic layers has also been used to track ocean circulation in the main ocean basins (e.g., in the World Ocean Circulation Experiment (WOCE)) and motivated the establishment of a specialized radiocarbon laboratory at the Woods Hole Oceanographic Institute (Jones et al., 1990). Techniques have been proposed to separate the bomb radiocarbon contribution from the natural background (e.g., Broecker et al., 1995; Rubin & Key, 2002), enabling the derivation of prebomb MRE values. For a more detailed discussion on bomb ^{14}C in the ocean, the reader is referred to Nydal (2000) and the papers generated by the GLODAP project (http://cdiac.ornl.gov/oceans/glodap/Radiocarbon.html).

11. Synthesis and Future Directions

Marine radiocarbon ages must be interpreted with care. Whereas calibration with global marine curves accounts for the global average of the MRE, research illustrates the necessity of taking into account local deviations from this mean. Where the magnitudes of these offsets are not large, the use of ΔR values may not always significantly influence a calibrated age but for most of the world regions these values are not negligible. The current paradigm of subtracting ΔR from marine radiocarbon ages prior calibration is the best approach available at present and softwares like OxCal (Bronk Ramsey, 2009) and CALIB (Stuiver & Reimer, 1986) are capable of taking into account ΔR values and their uncertainties—provided by the user—for the calibration of marine radiocarbon ages. The subtraction of ΔR can shift the radiocarbon age distribution from plateaus in the global curve, thereby increasing the precision of the obtained calibrated date. On the other hand, this process can equally shift the distribution so it intercepts a plateau but, in this case, the decrease in precision is accompanied by an increase in accuracy.

A discussion of the MRE requires the analysis of local ocean dynamics for these values are a product of the physical, chemical, and biological processes responsible for the uptake and distribution of radiocarbon in the heterogeneous marine realm. Marine radiocarbon ages interpretations cannot be decoupled from an assessment of local ocean regimes. This process is a mutual complementary relationship in which knowledge of the MRE can also lead to enhanced understanding of related marine phenomena. Since temporal and spatial variation may occur, marine radiocarbon ages must be interpreted in the light of oceanographic features and the ΔR values to calibrate these ages should be chosen after a careful analysis of the regional oceanography and its evolution over time. Even when choosing ΔR values from the interactive Marine Reservoir Database, the original publications in which they were derived should be read so the user can check samples and methods employed for their calculation.

Regarding the Marine Reservoir Database, it is important to remember that the data available are temporally limited and the addition of palaeovalues for the MRE would enhance the scientific contribution of the tool, making it more robust for scientists working in different time scales. For this purpose, the production of maps similar to Figure 7, showing the MRE at different time scales, would be an efficient and didactic way of displaying temporal fluctuations in the MRE for places where there are enough data and thus assisting in the visualization of changes in ocean dynamics. Moreover, discussions on oceanic configurations and climate changes known to have demonstrably changed the MRE would make the database even more practical. Notes by the authors of the original publications warning on very local hardwater and/or freshwater effects could also be added. Finally, regional means can be useful when statistical tests allow the combination of ΔR values, but this should be used with care due to the possibility of great variability within the same region. Here it is important to remember that enclosed in the same geographical region, there may be more than one ocean setting operating and that hardwater and/or freshwater effects can affect estuaries in an extremely local scale. Therefore, marking estuarine regions in the Marine Reservoir Database would also allow for a better sense of where riverine input is effectively influencing the MRE, ultimately affecting coastal studies.

After the recognition of the disequilibrium in radiocarbon content between atmosphere and oceans, the amount of research being published on the topic increased (Figure 6), yielding new data for different world regions and providing a better understanding of the time dependency of MREs. The quantification of this disequilibrium has been the main objective of many papers, which then use the MRE values as a proxy for changes in circulation, freshwater input and air-sea exchange, and/or for the correct calibration of marine ^{14}C ages. Radiocarbon MRE research is likely to expand in the next years as the ongoing climate change prompts the scientific community to look at the paleoclimate in search for clues about the behavior of the different components of Earth's climate system. In this context, marine reservoir ages have proven to be extremely useful proxies for processes such as ocean dynamics and air-sea interactions, establishing a link between the responses of the continental and marine realms to the onset of climatic events. Since accurate marine calibration depends upon MRE information, there is a considerable incentive for archeologists and archeological scientists to calculate the regional ΔR corrections for different world locations. Investment in MRE research has allowed reliable absolute chronologies to be constructed for coastal sites over the world and it seems likely that the calculation of radiocarbon MRE offsets will continue, as evidenced by the recent creation of new tools for this procedure (Reimer & Reimer, 2016; Soulet, 2015). Comprehensive local records, robust enough to deal with the MRE temporal variation, have not yet been used to assist in the construction of regional calibration curves. However, it is still possible the future development of regional calibration curves that will be useful in regions with particular ocean settings such as the Black and the Caspian Seas (Soulet, 2015). Advancements in pretreatments for the radiocarbon dating of carbonates, aiming to remove recrystallized phases (e.g., Douka et al., 2010), are also likely to improve the reliability of the next generation of calculated ΔR values. This, allied with the capacity to measure small quantities of material, allows for new sample possibilities and for new avenues of research for the MRE.

Acknowledgments
We are grateful to Paula and Ron Reimer, Katy Sparrow, Renan P. Cardoso, Fenix G. T. Kodovska, and Ingrid Chanca for helpful comments and discussions. We are also grateful to the anonymous reviewers whose insights improved this paper. We thank the Brazilian National Council for Scientific and Technological Development (CNPq) for financial support. The data that were used for this study are freely available at http://calib.qub.ac.uk/marine/.

References

Adkins, J. F., & Boyle, E. A. (1997). Changing atmospheric $\Delta^{14}C$ and the record of paleoventilation ages. *Paleoceanography*, *12*(3), 337–344.
Adkins, J. F. (1998). Deep-sea coral evidence for rapid change in ventilation of the deep North Atlantic 15,400 years ago. *Science*, *280*(5364), 725–728.
Aitken, M. (1990). *Science-based dating in archaeology* (294 pp.). London: Longman.
Albero, M. C., Angiolini, F. E., & Piana, E. (1986). Discordant ages related to reservoir effect of associated archaeologic remains from the Tunel Site, Beagle Channel, Argentine Republic. *Radiocarbon*, *28*(2), 748–753.
Anderson, E., & Libby, W. (1951). World-wide distribution of natural radiocarbon. *Physical Review*, *81*(1), 64–69.
Anderson, E. C., Libby, W. F., Weinhouse, S., Reid, A. F., Kirshenbaum, D., & Grosse, A. V. (1947). Natural radiocarbon from cosmic radiation. *Physical Review*, *72*(10), 931–936.
Andree, M., Oeschger, H., Broecker, W., Beavan, N., Klas, M., Mix, A., et al. (1986). Limits on the ventilation rate for the deep ocean over the last 12000 years. *Climate Dynamics*, *1*, 53–62.
Archer, D., Winguth, A., Lea, D., & Mahowald, N. (2000). What caused the glacial/interglacial atmospheric pCO_2 cycles? *Reviews of Geophysics*, *38*(2), 159–189. https://doi.org/10.1029/1999RG000066
Arneborg, J., Heinemeier, J., Lynnerup, N., Nielsen, H., Rud, N., & Sveinbjornsdottir, A. (1999). Change of diet of the Greenland Vikings determined from stable carbon analysis and ^{14}C dating of their bones. *Radiocarbon*, *41*(2), 157–168.
Arnold, J. R., & Libby, W. F. (1949). Age determinations by radiocarbon content: Checks with samples of known age. *Science*, *110*, 678–680.
Ascough, P., Cook, G., Dugmore, A., Barber, J., Higney, E., & Scott, E. M. (2004). Holocene variations in the Scottish Marine Radiocarbon Reservoir Effect. *Radiocarbon*, *46*(2), 611–620.
Ascough, P., Cook, G., & Dugmore, A. (2005). Methodological approaches to determining the marine radiocarbon reservoir effect. *Progress in Physical Geography: Earth and Environment*, *29*(4), 532–547.
Ascough, P., Cook, G., Dugmore, A., Scott, E., & Freeman, S. (2005). Influence of mollusc species on marine ΔR determinations. *Radiocarbon*, *47*(3), 433–440.

Ascough, P. L., Cook, G. T., Church, M. J., Dugmore, A. J., McGovern, T. H., Dunbar, E., et al. (2007). Reservoirs and radiocarbon: ^{14}C dating problems in Mývatnssveit, Northern Iceland. *Radiocarbon*, *49*(2), 947–961.
Ascough, P. L., Cook, G. T., Dugmore, A. J., & Scott, E. M. (2007). The North Atlantic marine reservoir effect in the Early Holocene: Implications for defining and understanding MRE values. *NIMB*, *259*, 438–447.
Ascough, P. L., Church, M. J., & Cook, G. T. (2017). Marine radiocarbon reservoir effects for the Mesolithic and Medieval Periods in the Western Isles of Scotland. *Radiocarbon*, *59*(01), 17–31.
Austin, W., Bard, E., Hunt, J., Kroon, D., & Peacock, J. (1995). The ^{14}C age of the Icelandic Vedde Ash: Implications for Younger Dryas marine reservoir age corrections. *Radiocarbon*, *37*(1), 53–62.
Bard, E. (1988). Correction of accelerator mass spectrometry ^{14}C ages measured in planktonic foraminifera: Paleoceanographic implications. *Paleoceanography*, *3*(6), 635–645.
Bard, E., Labeyrie, L., Arnold, M., Labracherie, M., Pichon, J. J., Duprat, J., & Duplessy, J. C. (1989). AMS-14C ages measured in deep sea cores from the Southern Ocean: Implications for sedimentation rates during isotope stage 2. *Quaternary Research*, *31*(2), 309–317. https://doi.org/10.1016/0033-5894(89)90011-2
Bard, E. (1998). Geochemical and geophysical implications of the radiocarbon calibration. *Geochimica et Cosmochimica Acta*, *62*(12), 2025–2038.
Bard, E., Arnold, M., Mangerud, J., Paterne, M., Labeyrie, L., Duprat, J., et al. (1994). The North Atlantic atmosphere-sea surface ^{14}C gradient during the Younger Dryas climatic event. *Earth and Planetary Science Letters*, *126*(4), 275–287. https://doi.org/10.1016/0012-821X(94)90112-0
Bard, E., Arnold, M., Hamelin, B., Tisnerat-Laborde, N., & Cabioch, G. (1998). Radiocarbon calibration by means of mass spectrometric ^{230}Th/^{234}U and ^{14}C ages of corals: An updated database including samples from Barbados, Mururoa and Tahiti. *Radiocarbon*, *40*(3), 1085–1092.
Beavan, N. R., & Sparks, R. J. (1998). Factors influencing ^{14}C ages of the Pacific rat Rattus exulans. *Radiocarbon*, *40*(2), 601–613.
Beavan-Athfield, N. R., McFadgen, B. G., & Sparks, R. J. (2001). Environmental influences on dietary carbon and ^{14}C ages in modern rats and other species. *Radiocarbon*, *43*(1), 7–14.
Bennett, C., Beukens, R., Clover, M., Gove, H., Liebert, R., Litherland, A., et al. (1977). Radiocarbon dating using electrostatic accelerators: Negative ions provide the key. *Science*, *198*, 508–510.
Berger, R., Taylor, R. E., & Libby, W. F. (1966). Radiocarbon content of marine shells from the California and Mexican West Coast. *Science*, *153*(3738), 864–6.
Berkman, P. A., & Forman, S. L. (1996). Pre-bomb radiocarbon and the reservoir correction for calcareous marine species in the Southern Ocean. *Geophysical Research Letters*, *23*(4), 363–366.
Bethe, H. A., Korff, S. A., & Placzek, G. (1940). On the interpretation of neutron measurements in cosmic radiation. *Physical Review*, *57*(7), 573–587.
Björck, S., Koç, N., & Skog, G. (2003). Consistently large marine reservoir ages in the Norwegian Sea during the Last Deglaciation. *Quaternary Science Reviews*, *22*(5–7), 429–435. https://doi.org/10.1016/S0277-3791(03) 00002-7
Blau, M., Deevey, E. S., & Gross, M. S. (1953). Yale natural radiocarbon measurements, I. Pyramid Valley, New Zealand, and its problems. *Science*, *118*, 1–6.
Blockley, S. P. E., & Housley, R. A. (2009). Calibration commentary. *Radiocarbon*, *51*(1), 287–290.
Bolin, B., & Fung, I. (1992). Report: The carbon cycle revisited. *Modeling the Earth system*, *3*, 151–164.
Bolton, A., Goodkin, N. F., Druffel, E. R. M., Griffin, S., & Murty, S. A. (2016). Upwelling of Pacific intermediate water in the South China Sea revealed by coral radiocarbon record. *Radiocarbon*, *58*(01), 37–53. https://doi.org/10.1017/RDC.2015.4
Bondevik, S., Mangerud, J., Birks, H., Gulliksen, S., & Reimer, P. (2006). Changes in North Atlantic radiocarbon reservoir ages during the Allerod and Younger Dryas. *Science*, *312*, 1514–1517.
Bowman, G. (1985). Oceanic reservoir correction for marine radiocarbon dates from Northwestern Australia. *Australian Archaeology*, *6*(20), 58–67.
Bowman, G., & Harvey, N. (1983). Radiocarbon dating marine shells in South Australia. *Australian Archaeology*, *12*(17), 113–123.
Broecker, W (1991). The great ocean conveyor. *Oceanography*, *4*(2), 79–89.
Broecker, W., Gerard, R., Ewing, M., & Heezen, B. (1960). Natural radiocarbon in the Atlantic Ocean. *Journal of Geophysical Research*, *65*(9), 2903–2931.
Broecker, W., Mix, A., Andree, M., & Oeschger, H. (1984). Radiocarbon measurements on coexisting benthic and planktic foraminifera shells: Potential for reconstructing ocean ventilation times over the past 20 000 years. *Nuclear Instruments and Methods in Physics Research B*, *5*(2), 331–339.
Broecker, W., Peteet, D., & Rind, D. (1985). Does the ocean-atmosphere system have more than one stable mode of operation? *Nature*, *315*, 21–26.
Broecker, W. S., Andree, M., Bonani, G., Wolfli, W., Oeschger, H., Klas, M., et al. (1988). Preliminary estimates for the radiocarbon age of deep water in the glacial ocean. *Paleoceanography*, *3*(6), 659–669.
Broecker, W. S., Sutherland, S., & Smethie, W. (1995). Oceanic radiocarbon: Separation of the natural and bomb components. *Global Biogeochemical Cycles*, *9*(2), 263–288.
Broecker, W. S., Clark, E., Hajdas, I., & Bonani, G. (2004). Glacial ventilation rates for the deep Pacific Ocean. *Paleoceanography*, *19*, PA2002. https://doi.org/10.1029/2003PA000974
Broecker, W., & Barker, S. (2007). A 190‰ drop in atmosphere's Δ^{14}C during the "Mystery Interval" (17.5 to 14.5 kyr). *Earth and Planetary Science Letters*, *256*(1-2), 90–99.
Broecker, W. S., Denton, G. H., Edwards, R. L., Cheng, H., Alley, R. B., & Putnam, A. E. (2010). Putting the Younger Dryas cold event into context. *Quaternary Science Reviews*, *29*(9-10), 1078–1081.
Bronk Ramsey, C. (2008). Radiocarbon dating: Revolutions in understanding. *Archaeometry*, *50*(2), 249–275.
Bronk Ramsey, C. (2009). Bayesian analysis of radiocarbon dates. *Radiocarbon*, *51*(1), 337–360.
Bronk Ramsey, C., & Lee, S. (2013). Recent and planned developments of the Program OxCal. *Radiocarbon*, *55*(2), 720–730.
Bruns, M., Levin, I., Munnich, K., Hubberten, H. H., & Fillipakis, S. (1980). Regional sources of volcanic carbon dioxide and their influence on ^{14}C content of present-day plant material. *Radiocarbon*, *22*(2), 532–536.
Burke, A., Stewart, A., Adkins, J., Ferrari, R., Jansen, M., & Thompson, A. (2015). The glacial mid-depth radiocarbon bulge and its implications for the overturning circulation. *Paleoceanography*, *30*, 1021–1039. https://doi.org/10.1002/2015PA002778
Burr, G., Haynes, G., Shen, C., Taylor, F., Chang, Y., Beck, J., et al. (2015). Temporal variations of radiocarbon reservoir ages in the South Pacific ocean during the Holocene. *Radiocarbon*, *57*(4), 507–515.

Butler, P. G., Scourse, J. D., Richardson, C. A., Wanamaker, A. D., Bryant, C. L., & Bennell, J. D. (2009). Continuous marine radiocarbon reservoir calibration and the ^{13}C Suess effect in the Irish Sea: Results from the first multi-centennial shell-based marine master chronology. *Earth and Planetary Science Letters*, *279*(3-4), 230–241.

Butzin, M., Prange, M., & Lohmann, G. (2005). Radiocarbon simulations for the glacial ocean: The effects of wind stress, Southern Ocean sea ice and Heinrich events. *Earth and Planetary Science Letters*, *235*(1–2), 45–61.

Butzin, M., Köhler, P., & Lohmann, G. (2017). Marine radiocarbon reservoir age simulations for the past 50,000 years. *Geophysical Research Letters*, *44*, 8473–8480. https://doi.org/10.1002/2017GL074688

Campbell, M. J., Farmer, J. C., Fitzner, C. A., Henry, M. N., Sheppard, J. C., Hardy, R. J., et al. (1986). Radiocarbon tracer measurements of atmospheric hydroxyl radical concentrations. *Journal of Atmospheric Chemistry*, *4*, 413–427. https://doi.org/10.1007/BF00053843

Carré, M., Jackson, D., Maldonado, A., Chase, B. M., & Sachs, J. P. (2016). Variability of ^{14}C reservoir age and air-sea flux of CO_2 in the Peru-Chile upwelling region during the past 12,000 years. *Quaternary Research (United States)*, *85*(1), 87–93.

Clark, J. T., Quintus, S., Weisler, M. I., Pierre, E. S., Nothdurft, L., Feng, Y., & Hua, Q. (2016). Marine reservoir correction for American Samoa using U-series and AMS dated corals. *Radiocarbon*, *58*(4), 851–868.

Clarke, E. T., & Korff, S. A. (1941). The radiosonde: The stratosphere laboratory. *Journal of The Franklin Institute*, *232*(4), 339–355.

Clilverd, M., Clarke, E., Rishbeth, H., Clarck, T., & Ulich, T. (2003). Solar activity levels in 2100. *Astronomy & Geophysics*, *44*, 5.20–5.22.

Clilverd, M., Clarke, E., Clark, T., Rishbeth, H., & Ulich, T. (2004). … and a reply. *Astronomy and Geophysics*, *45*(2), 7.

Commendador, A. (2014). Radiocarbon dating human skeletal material on Rapa Nui: Evaluating the effect of uncertainty in marine-derived carbon. *Radiocarbon*, *56*(1), 277–294.

Cook, G. T., Scott, E. M., & Harkness, D. D. (2009). Radiocarbon as a tracer in the global carbon cycle. *Radioactivity in the Environment*, *16*, 89–137.

Cook, G. T., Ascough, P. L., Bonsall, C., Hamilton, W. D., Russell, N., Sayle, K. L., et al. (2015). Best practice methodology for ^{14}C calibration of marine and mixed terrestrial/marine samples. *Quaternary Geochronology*, *27*, 164–171.

Cook, M. S., & Keigwin, L. D. (2015). Radiocarbon profiles of the NW Pacific from the LGM and deglaciation: Evaluating ventilation metrics and the effect of uncertain surface reservoir ages. *Paleoceanography*, *30*, 174–195. https://doi.org/10.1002/2014PA002649

Craig, H (1953). The geochemistry of the stable carbon isotopes. *Geochimica et Cosmochimica Acta*, *3*, 53–92.

Craig, H. (1954). Carbon 13 in plants and the relationships between carbon 13 and carbon 14 variations in nature. *The Journal of Geology*, *62*(2), 115–149.

Craig, H (1957). The natural distribution of radiocarbon and the exchange time of carbon dioxide between atmosphere and sea. *Tellus A*, *9*(I), 1–17.

Culleton, B. J., Kennett, D. J., Ingram, B. L., Erlandson, J. M., & Southon, J. R. (2006). Intrashell radiocarbon variability in marine mollusks. *Radiocarbon*, *48*(3), 387–400.

Damon, P. E., & Peristykh, A. N. (2000). Radiocarbon calibration and application to geophysics, solar physics, and astrophysics. *Radiocarbon*, *42*(1), 137–150.

de la Fuente, M., Skinner, L., Calvo, E., Pelejero, C., & Cacho, I. (2015). Increased reservoir ages and poorly ventilated deep waters inferred in the glacial eastern equatorial Pacific. *Nature Communications*, *6*, 7420. https://doi.org/10.1038/ncomms8420

de Vries, H. (1958). Variation in concentration of radiocarbon with time and location on Earth, *Proceedings of the Koninklijke Nederlandse Akademie Van Weten- schappen* (Vol. B61, pp. 94–102), Series B-Palaeontology Geology Physics Chemistry Anthropology: Akademie Van Wet.

Deevey, E. S., Gross, M. S., Hutchinson, G. E., & Kraybill, H. L. (1954). The natural ^{14}C contents of materials from hard-water lakes. *Geology*, *40*, 285–288.

del Giorgio, P. A., & Duarte, C. M. (2002). Respiration in the open ocean. *Nature*, *420*(6914), 379–384.

Deo, J. N., Stone, J. O., & Stein, J. K. (2004). Building confidence in shell: Variations in the marine radiocarbon reservoir correction for the Northwest Coast over the past 3, 000 years. *American Antiquity*, *69*(4), 771–786.

Dettman, D., Mitchell, D., Huckleberry, G., & Foster, M. (2015). ^{14}C and marine reservoir effect in archaeological samples from the Northeast Gulf of California. *Radiocarbon*, *57*(5), 785–793.

Doney, S. C., Fabry, V. J., Feely, R. A., & Kleypas, J. A. (2009). Ocean acidification: The other CO_2 problem. *Annual Review of Marine Science*, *1*(1), 169–192.

Douarin, M., Elliot, M., Noble, S., Moreton, S., Long, D., Sinclair, D., et al. (2016). North Atlantic ecosystem sensitivity to Holocene shifts in Meridional overturning circulation. *Geophysical Research Letters*, *43*, 291–298. https://doi.org/10.1002/2015GL065999

Douka, K., Hedges, R. M., & Higham, T. G. (2010). Improved AMS ^{14}C dating of shell carbonates using high-precision X-Ray diffraction and a novel density separation protocol (CarDS). *Radiocarbon*, *52*(2), 735–751.

Druffel, E., & Suess, H. (1983). On the radiocarbon record in banded Corals: Exchange parameters and net transport of $^{14}CO_2$ between atmosphere and surface ocean. *Journal of Geophysical Research*, *88*(C2), 1271–1280.

Druffel, E. R. M., & Griffin, S. (1993). Large variations of surface ocean radiocarbon: Evidence of circulation changes in the southwestern Pacific. *Journal of Geophysical Research*, *98*(C11), 20,249–20,259. https://doi.org/10.1029/93JC02113

Druffel, E. R. M., & Griffin, S. (1999). Variability of surface ocean radiocarbon and stable isotopes in the southwestern Pacific. *Journal of Geophysical Research*, *104*(C10), 23,607–23,613.

Druffel, E. R., Robinson, L. F., Griffin, S., Halley, R. B., Southon, J. R., & Adkins, J. F. (2008). Low reservoir ages for the surface ocean from mid-Holocene Florida corals. *Paleoceanography*, *23*, PA2209. https://doi.org/10.1029/2007PA001527

Druffel, E., Griffin, S., Honjo, S., & Manganini, S. (1998). Evidence of old carbon in the deep water column of the Panama Basin from natural radiocarbon measurements. *Geophysical Research Letters*, *25*(10), 1733–1736.

Druffel, E. R. M. (1997). Pulses of rapid ventilation in the North Atlantic surface ocean during the past century. *Science*, *275*(5305), 1454–1457.

Druffel, E. R. M., Williams, P., Robertson, K., Griffin, S., Jull, A., Donahue, D., et al. (1989). Radiocarbon in dissolved organic and inorganic carbon from the central North Pacific. *Radiocarbon*, *31*(3), 523–532.

Dye, T. (1994). Apparent ages of marine shells: Implications for archaeological dating in Hawaii. *Radiocarbon*, *36*(1), 51–57.

Edinborough, K., Martindale, A., Cook, G. T., Supernant, K., & Ames, K. M. (2016). A marine reservoir effect ΔR Value for Kitandach, in Prince Rupert Harbour, British Columbia, Canada. *Radiocarbon*, *58*, 885–891.

Edwards, R. L., Beck, J. W., Burr, G. S., Donahue, D. J., Bloom, A. L., Druffel, E. R. M., & Taylor, F. W. (1993). A large drop in atmospheric $^{14}C/^{12}C$ and reduced melting in the Younger Dryas, documented with ^{230}Th ages of corals. *Science*, *260*(5), 962–968.

Eiríksson, J., Larsen, G., Knudsen, K. L., Heinemeier, J., & Símonarson, L. A. (2004). Marine reservoir age variability and water mass distribution in the Iceland Sea. *Quaternary Science Reviews*, *23*(20–22), 2247–2268.

England, M. H. (1995). The age of water and ventilation timescales in a global ocean model. *Journal of Physical Oceanography*, *25*, 2756–2777.
England, M. H., & Maier-Reimer, E. (2001). Using chemical tracers to assess ocean models. *Reviews of Geophysics*, *39*(1), 29–70. https://doi.org/10.1029/1998RG000043
Erlandson, J. M., Rick, T. C., Braje, T. J., Steinberg, A., & Vellanoweth, R. L. (2008). Human impacts on ancient shellfish: A 10,000 year record from San Miguel Island, California. *Journal of Archaeological Science*, *35*(8), 2144–2152.
Ervynck, A. (2014). Dating human remains from the historical period in Belgium: Diet changes and the impact of marine and freshwater reservoir effects. *Radiocarbon*, *56*(2), 779–788.
Facorellis, Y. (1998). Apparent ^{14}C ages of marine mollusk shells from a Greek Island: Calculation of the marine reservoir effect in the Aegean Sea. *Adiocarbon*, *40*(2), 963–973.
Facorellis, Y., & Vardala-Theodorou, E. (2015). Sea surface radiocarbon reservoir age changes in the Aegean Sea from about 11,200 BP to present. *Radiocarbon*, *57*(3), 493–505.
Fairbanks, R. G., Mortlock, R. A., Chiu, T. C., Cao, L., Kaplan, A., Guilderson, T. P., et al. (2005). Radiocarbon calibration curve spanning 0 to 50,000 years BP based on paired $^{230}Th/^{234}U/^{238}U$ and ^{14}C dates on pristine corals. *Quaternary Science Reviews*, *24*, 1781–1796.
Faivre, S., Bakran-Petricioli, T., Baresic, J., & Horvatincic, N. (2015). New data on marine radiocarbon effect in the eastern adriatic based on pre-bomb marine organisms from the intertidal zone and shallow sea. *Radiocarbon*, *57*(4), 527–538.
Falkowski, P., Scholes, R. J., Boyle, E., Canadell, J., Canfield, D., Elser, J., et al. (2000). The global carbon cycle: A test of our knowledge of Earth as a system. *Science*, *290*(5490), 291–296.
Fernandes, R., Millard, A. R., Brabec, M., Nadeau, M. J., & Grootes, P. (2014). Food reconstruction using isotopic transferred signals (FRUITS): A Bayesian model for diet reconstruction. *PLOS ONE*, *9*(2), 1–9.
Fifield, L. K. (1999). Accelerator mass spectrometry and its applications. *Reports on Progress in Physics*, *62*, 1223–1274.
Fifield, L. K. (2004). Applications of accelerator mass spectrometry: Advances and innovation. *Nuclear Instruments and Methods in Physics Research, Section B: Beam Interactions with Materials and Atoms*, *223–224*, 401–411.
Forman, S. L., & Polyak, L. (1997). Radiocarbon content of pre-bomb marine mollusks and variations in the ^{14}C reservoir age for coastal areas of the Barents and Kara seas Russia. *Geophysical Research Letters*, *24*(8), 885–888.
Friederich, G. E., Ledesma, J., Ulloa, O., & Chavez, F. P. (2008). Air-sea carbon dioxide fluxes in the coastal southeastern tropical Pacific. *Progress in Oceanography*, *79*(2-4), 156–166.
Galli, I., Bartalini, S., Ballerini, R., Barucci, M., Cancio, P., De Pas, M., et al. (2016). Spectroscopic detection of radiocarbon dioxide at parts-per-quadrillion sensitivity. *Optica*, *3*, 385.
Galli, I., Bartalini, S., Borri, S., Cancio, P., Mazzotti, D., De Natale, P., & Giusfredi, G. (2011). Molecular gas sensing below parts per trillion: Radiocarbon-dioxide optical detection. *Physical Review Letters*, *107*(27), 1–4.
Galli, I., Bartalini, S., Cancio, P., De Natale, P., Mazzotti, D., Giusfredi, G., et al. (2013). Optical Detection of Radiocarbon Dioxide: First Results and AMS Intercomparison. *Radiocarbon*, *55*, 213.
Gaudinski, J. B., Trumbore, S. E., Davidson, E. A., & Zheng, S. (2000). Soil carbon cycling in a temperate forest: Radiocarbon-based estimates of residence times, sequestration rates and partitioning of fluxes. *Biogeochemistry*, *51*, 33–69.
Geiger, H., & Müller, W. (1929). Technische Bemerkungen zum Elektronenzählorohr. *Physikalische Zeitschrift*, *30*, 489–493.
Gillespie, R. (1984). *Radiocarbon user's handbook*. Oxford: University of Oxford.
Godwin, H. (1951). Comments on radiocarbon dating for samples from the British Isles. *American Journal of Science*, *249*, 301–307.
Goldstein, S. J., Lea, D. W., Chakraborty, S., Kashgarian, M., & Murrell, M. T. (2001). Uranium-series and radiocarbon geochronology of deep-sea corals: Implications for Southern Ocean ventilation rates and the oceanic carbon cycle. *Earth and Planetary Science Letters*, *193*, 167–182. https://doi.org/10.1016/S0012-821X(01)00494-0
Gordon, J. E., & Harkness, D. D. (1992). Magnitude and geographic variation of the radiocarbon content in Antarctic marine life: Implications for reservoir corrections in radiocarbon dating. *Quaternary Science Reviews*, *11*, 697–708.
Gosse, J. C., & Phillips, F. M. (2001). Terrestrial in situ cosmogenic nuclides: Theory and application. *Quaternary Science Reviews*, *20*, 1475–1560.
Gröcke, D. R., & Gillikin, D. P. (2008). Advances in mollusc sclerochronology and sclerochemistry: Tools for understanding climate and environment. *Geo-Marine Letters*, *28*(5-6), 265–268.
Hadden, C., & Cherkinsky, A. (2015). ^{14}C variations in pre-bomb nearshore habitats of the Florida Panhandle, USA. *Radiocarbon*, *57*(3), 469–479.
Hadden, C. S., & Cherkinsky, A. (2017). Spatiotemporal variability in ΔR in the Northern Gulf of Mexico, USA. *Radiocarbon*, *59*(2). https://doi.org/10.1017/RDC.2016.65
Hajdas, I. (2008). Radiocarbon dating and its applications in Quaternary studies. *Quaternary Science Journal*, *57*, 2–24.
Hales, B., Takahashi, T., & Bandstra, L. (2005). Atmospheric CO_2 uptake by a coastal upwelling system. *Global Biogeochemical Cycles*, *19*, GB1009. https://doi.org/10.1029/2004GB002295
Hall, B. L., Henderson, G. M., Baroni, C., & Kellogg, T. B. (2010). Constant Holocene Southern-Ocean ^{14}C reservoir ages and ice-shelf flow rates. *Earth and Planetary Science Letters*, *296*(1–2), 115–123.
Head, J., Jones, R., & Allen, J. (2016). Calculation of the "Marine Reservoir Effect" from the dating of shell-charcoal paired samples from an Aboriginal Midden on Great Glennie Island, Bass Strait. *Australian Archaeology*, *12*(17), 99–112.
Heier-Nielsen, S., Heinemeier, J., Nielsen, H. L., & Rud, N. (1995). Recent reservoir ages for Danish fjords and marine waters. *Radiocarbon*, *37*(3), 875–882.
Herndl, G. J., & Reinthaler, T. (2013). Microbial control of the dark end of the biological pump. *Nature Geoscience*, *6*(9), 718–724.
Hesshaimer, V., Heimann, M., & Levin, I. (1994). Radiocarbon evidence for a smaller oceanic carbon dioxide sink than previously believed. *Nature*, *370*, 201–203.
Higham, T., & Hogg, A. (1995). Radiocarbon dating of prehistoric shell from New Zealand and calculation of the ΔR value using fish otoliths.*Radiocarbon*, *37*(2), 409–416.
Hines, S. K. V., Southon, J. R., & Adkins, J. F. (2015). A high-resolution record of Southern Ocean intermediate water radiocarbon over the past 30,000 years. *Earth and Planetary Science Letters*, *432*, 46–58.
Hinojosa, J. L., Moy, C. M., Prior, C. A., Eglinton, T. I., McIntyre, C. P., Stirling, C. H., & Wilson, G. S. (2015). Investigating the influence of regional climate and oceanography on marine radiocarbon reservoir ages in southwest New Zealand. *Estuarine, Coastal and Shelf Science*, *167*, 526–539.
Hjort, C. (1973). A sea correction for East Greenland. *Geologiska Foreningen i Stockholm Forhandlingar*, *95*(1), 132–134.
Hogg, A., Higham, T. F., & Dahm, J. (1998). ^{14}C dating of modern marine and estuarine shellfish. *Radiocarbon*, *40*(2), 975–984.

Hogg, A., Palmer, J., Boswijk, G., & Turney, C. (2011). High-precision radiocarbon measurements of tree-ring dated wood from New Zealand: 195 BC–AD 995. *Radiocarbon*, *53*(3), 529–542.
Hogg, A., Hua, Q., Blackwell, P. G., Niu, M., Buck, C. E., Guilderson, T. P., et al. (2013). SHCal13 Southern Hemisphere calibration, 0–50,000 years cal BP. *Radiocarbon*, *55*(4), 1889–1903.
Hua, Q. (2009). Radiocarbon: A chronological tool for the recent past. *Quaternary Geochronology*, *4*(5), 378–390.
Hua, Q., Barbetti, M., & Rakowski, A. Z. (2013). Atmospheric radiocarbon for the period 1950–2010. *Radiocarbon*, *55*(4), 2059–2072.
Hua, Q., Webb, G. E., xin Zhao, J., Nothdurft, L. D., Lybolt, M., Price, G. J., & Opdyke, B. N. (2015). Large variations in the Holocene marine radiocarbon reservoir effect reflect ocean circulation and climatic changes. *Earth and Planetary Science Letters*, *422*, 33–44.
Hudson, J. H., Shinn, E. A., Halley, R. B., & Lidz, B. (1976). Sclerochronology: A tool for interpreting past environments. *Geology*, *4*(6), 361–364.
Hughen, K. A., Overpeck, J. T., Lehman, S. J., Kashgarian, M., Southon, J., Peterson, L. C., et al. (1998). Deglacial changes in ocean circulation from an extended radiocarbon calibration. *Nature*, *391*, 65–68.
Hughen, K. A., Baillie, M. G. L., Bard, E., Beck, J. W., Bertrand, C. J. H., Blackwell, P. G., et al. (2004). Marine04 marine radiocarbon age calibration, 0–26 cal kyr BP. *Radiocarbon*, *46*(3), 1059–1066.
Huyer, A. (1983). Coastal upwelling in the California current system. *Progress in Oceanography*, *12*(3), 259–284. https://doi.org/10.1016/0079-6611(83)90010-1
Ikehara, K., Danhara, T., Yamashita, T., Tanahashi, M., Morita, S., & Ohkushi, K. (2011). Paleoceanographic control on a large marine reservoir effect offshore of Tokai, south of Japan, NW Pacific, during the last glacial maximum-deglaciation. *Quaternary International*, *246*(1–2), 213–221. https://doi.org/10.1016/j.quaint.2011.07. 005
Ingram, B. L., & Southon, J. R. (1996). Reservoir ages in eastern Pacific coastal and estuarine waters. *Radiocarbon*, *38*, 573–582.
Jones, G. A., McNichol, A. P., von Reden, K. F., & Schneider, R. J. (1990). The National Ocean Sciences AMS facility at Woods Hole Oceanographic Institution. *Nuclear Instruments and Methods in Physics Research Section B: Beam Interactions with Materials and Atoms*, *52*(3-4), 278–284.
Jones, K. B., Hodgins, G. W. L., Dettman, D. L., Andrus, C. F. T., Nelson, A., & Etayo-Cadavid, M. F. (2007). Seasonal variations in Peruvian marine reservoir age from pre-bomb Argopecten Purpuratus shell carbonate. *Radiocarbon*, *49*(2), 877–888.
Jong, A. D., & Mook, W. (1982). An anomalous Suess effect above Europe. *Nature*, *298*, 641–644.
Joos, F. (1999). Global warming and marine carbon cycle feedbacks on future atmospheric CO_2. *Science*, *284*(5413), 464–467.
Keigwin, L. D. (2004). Radiocarbon and stable isotope constraints on Last Glacial Maximum and Younger Dryas ventilation in the western North Atlantic. *Paleoceanography*, *19*, PA4012. https://doi.org/10.1029/2004PA001029
Kennett, D., Ingram, B., Erlandson, J., & Walker, P. (1997). Evidence for temporal fluctuations in marine radiocarbon reservoir ages in the Santa Barbara Channel, Southern California. *Journal of Archaeological Science*, *24*, 1051–1059.
Khatiwala, S., Primeau, F., & Holzer, M. (2012). Ventilation of the deep ocean constrained with tracer observations and implications for radiocarbon estimates of ideal mean age. *Earth and Planetary Science Letters*, *325–326*, 116–125. https://doi.org/10.1016/j.epsl. 2012.01.038
Komugabe, A. F., Fallon, S. J., Thresher, R. E., & Eggins, S. M. (2014). Modern Tasman Sea surface reservoir ages from deep-sea black corals. *Deep-Sea Research Part II: Topical Studies in Oceanography*, *99*, 207–212.
Komugabe-Dixson, A. F., Fallon, S. J., Eggins, S. M., & Thresher, R. E. (2016). Radiocarbon evidence for mid-late Holocene changes in southwest Pacific Ocean circulation. *Paleoceanography*, *31*, 971–985. https://doi.org/10.1002/2016PA002929
Korff, S. (1939). Recent studies at high elevations. *Reviews of Modern Physics*, *11*, 211.
Korff, S., & Clarke, E. (1942). The production of neutrons and protons by the cosmic radiation at 14,125 feet. *Physical Review*, *61*, 1941.
Korff, S., & Hamermesh, B. (1946). The energy distribution and number of cosmic-ray neutrons in the free atmosphere. *Physical Review*, *69*(5–6), 155.
Korff, S. A., & Mendell, R. B. (1980). Variations in radiocarbon production in the Earth's atmosphere. *Radiocarbon*, *22*(2), 159–165.
Kovanen, D. J., & Easterbrook, D. J. (2002). Paleodeviations of radiocarbon marine reservoir values for the northeast Pacific. *Geology*, *30*(3), 243–246.
Kulp, J. L., Tryon, L. E., Eckelman, W. R., & Snell, W. A. (1952). Lamont natural radiocarbon measurements, II. *Science*, *116*, 409–414.
Kuzmin, Y. V., Nevesskaya, L. A., Krivonogov, S. K., & Burr, G. S. (2007). Apparent ^{14}C ages of the "pre-bomb" shells and correction values (R, ΔR) for Caspian and Aral Seas (Central Asia). *Nuclear Instruments and Methods in Physics Research Section B: Beam Interactions with Materials and Atoms*, *259*(1), 463–466.
Lal, D. (1988). In situ-produced cosmogenic isotopes in terrestrial rocks. *Annual Review of Earth and Planetary Sciences*, *16*, 355–388.
Lal, D., & Jull, a. J. T. (2001). In-situ cosmogenic ^{14}C: Production and examples of its unique applications in studies of terrestrial and extraterrestrial processes. *Radiocarbon*, *43*(2B), 731–742.
Lal, D., & Peters, B. (1967). Cosmic ray produced radioactivity on the Earth. In K. Sitte (Ed.), *Kosmische Strahlung II/Cosmic Rays II* (Vol. 9 / 46 / 2, pp. 551–612). Berlin: Springer. https://doi.org/10.1007/978-3-642-46079-1
Latorre, C., De Pol-Holz, R., Carter, C., & Santoro, C. M. (2017). Using archaeological shell middens as a proxy for past local coastal upwelling in northern Chile. *Quaternary International*, *427*, 128–136.
Le Quéré, C., Raupach, M. R., Canadell, J. G., & Marland, G. (2009). Trends in the sources and sinks of carbon dioxide. *Nature Geoscience*, *2*(12), 831–836.
Le Quéré, C., Rödenbeck, C., Buitenhuis, E. T., Conway, T. J., Langenfelds, R., Gomez, A., et al. (2007). Saturation of the Southern Ocean CO_2 sink due to recent climate change. *Science*, *316*, 1735–1738.
Lerman, J., Mook, W., & Vogel, J. (1970). ^{14}C in tree rings from different localities, and absolute chronology. In *Proceedings, XII Nobel Symposium* (pp. 275–301). New York.
Levin, I., & Hesshaimer, V. (2000). Radiocarbon—A unique tracer of global carbon cycle dynamics. *Radiocarbon*, *42*(1), 69–80.
Levin, I., Kromer, B., Wagenbach, D., & Münnich, K. (1987). Carbon isotope measurements of atmospheric CO_2 at a coastal station in Antarctica. *Tellus B*, *39B*, 89–95.
Levin, I., Schuchard, J., Kromer, B., & Münnich, K. (1989). The continental European Suess effect. *Radiocarbon*, *31*(3), 431–440.
Libby, W., Anderson, E., & Arnold, J. (1949). Age determination by radiocarbon content: World-wide assay of natural radiocarbon. *Science*, *109*, 227–228.
Libby, W. F. (1934). Radioactivity of neodymium and samarium. *Physical Review*, *46*, 196.
Libby, W. F. (1946). Atmospheric helium three and radiocarbon from cosmic radiation. *Physical Review*, *69*, 671–672.
Lindsay, C. M., Lehman, S. J., Marchitto, T. M., & Ortiz, J. D. (2015). The surface expression of radiocarbon anomalies near Baja California during deglaciation. *Earth and Planetary Science Letters*, *422*, 67–74.
Lingenfelter, R. E. (1963). Production of Carbon 14 by cosmic-ray neutrons. *Review of Geophysics*, *1*(1), 35–55.

Little, E. A. (1993). Radiocarbon age calibration at archaeological sites of coastal Massachusetts and vicinity. *Journal of Archaeological Science*, *20*, 457–471.
Lougheed, B. C., van der Lubbe, H. J. L., & Davies, G. R. (2016). $^{87}Sr/^{86}Sr$ as a quantitative geochemical proxy for 14C reservoir age in dynamic, brackish waters: Assessing applicability and quantifying uncertainties. *Geophysical Research Letters*, *43*, 735–742. https://doi.org/10.1002/2015GL066983
Lougheed, B. C., Filipsson, H. L., & Snowball, I. (2013). Large spatial variations in coastal ^{14}C reservoir age—A case study from the Baltic Sea. *Climate of the Past*, *9*(3), 1015–1028.
Lowe, D. J. (2011). Tephrochronology and its application: A review. *Quaternary Geochronology*, *6*(2), 107–153.
Macario, K. D., Alves, E. Q., Carvalho, C., Oliveira, F. M., Ramsey, C. B., Chivall, D., et al. (2016). The use of the terrestrial snails of the genera Megalobulimus and Thaumastus as representatives of the atmospheric carbon reservoir. *Scientific Reports*, *6*, 27395.
Macario, K. D., Alves, E. Q., Chanca, I. S., Oliveira, F. M., Carvalho, C., Souza, R., et al. (2016). The Usiminas shellmound on the Cabo Frio Island: Marine reservoir effect in an upwelling region on the coast of Brazil. *Quaternary Geochronology*, *35*, 36–42.
Macario, K. D., Souza, R. C. C. L., Aguilera, O. A., Carvalho, C., Oliveira, F. M., Alves, E. Q., et al. (2015). Marine reservoir effect on the Southeastern coast of Brazil: Results from the Tarioba shellmound paired samples. *Journal of Environmental Radioactivity*, *143*, 14–19.
Mangerud, J. (1972). Radiocarbon dating of marine shells including a discussion of the apparent age of recent shells from Norway. *Boreas*, *1*(l), 143–172.
Mangerud, J., & Gulliksen, S. (1975). Apparent radiocarbon ages of recent marine shells from Norway, Spitsbergen, and Arctic Canada. *Quaternary Research*, *5*(2), 263–273.
Marchitto, T. M., Jones, G. A., Goodfriend, G. A., & Weidman, C. R. (2000). Precise temporal correlation of Holocene mollusk shells using sclerochronology. *Quaternary Research*, *53*(2), 236–246.
Marchitto, T. M., Lehman, S. J., Ortiz, J. D., Fluckiger, J., & van Geen, A. (2007). Marine radiocarbon evidence for the mechanism of deglacial atmospheric CO_2 Rise. *Science*, *316*(5830), 1456–1459. https://doi.org/10.1126/science.1138679
Martins, J. M. M. (2013). Marine radiocarbon reservoir effect in Southern Atlantic Iberian Coast. *Radiocarbon*, *55*(2), 1123–1134.
Masarik, J., & Beer, J. (1999). Simulation of particle fluxes and cosmogenic nuclide production in the Earth's atmosphere. *Journal of Geophysical Research*, *104*(D10), 12,099–12,111.
Masuda, K., Nagaya, K., Miyahara, H., Muraki, Y., & Nakamura, T. (2009). Cosmogenic radiocarbon and the solar activity. *Journal of the Physical Society of Japan*, *78*, 1–6.
McCormac, F. G., Hogg, A. G., Higham, F. G., Baillie, G. L., Palmer, J. G., Xiong, L., et al. (1998). Variations of radiocarbon in tree rings: Southern Hemisphere offset preliminary results. *Radiocarbon*, *40*(3), 1153–1159.
McCormac, F. G., Reimer, P. J., Hogg, A. G., Higham, T. F. G., Baillie, M. G. L., Palmer, J., & Stuiver, M. (2002). Calibration of the radiocarbon time scale for the Southern Hemisphere: AD 1850–950. *Radiocarbon*, *44*(3), 641–651.
McElroy, M. B. (1983). Marine biological controls on atmospheric CO_2 and climate. *Nature*, *302*(3), 328–329.
McFadgen, B. (1982). Dating New Zealand archaeology by radiocarbon. *New Zealand Journal of Science*, *25*, 379–392.
McGregor, H. V., Gagan, M. K., McCulloch, M. T., Hodge, E., & Mortimer, G. (2008). Mid-Holocene variability in the marine ^{14}C reservoir age for northern coastal Papua New Guinea. *Quaternary Geochronology*, *3*(3), 213–225.
Merlivat, L., & Memery, L. (1983). Gas exchange across an air-water interface: Experimental results and modeling of bubble contribution to transfer. *Journal of Geophysical Research*, *88*, 707–724.
Mills, G. A., & Urey, H. C. (1940). The kinetics of isotopic exchange between carbon dioxide, bicarbonate ion, carbonate ion and water. *Journal of the American Chemical Society*, *62*, 1019–1026.
Monge Soares, A. M., Gutiérrez-Zugasti, I., González-Morales, M., Matos Martins, J. M., Cuenca-Solana, D., & Bailey, G. N. (2016). Marine radiocarbon reservoir effect in late Pleistocene and early Holocene coastal waters off Northern Iberia. *Radiocarbon*, *58*, 869–883.
Montgomery, C., & Montgomery, D. (1939). The intensity of neutrons of thermal energy in the atmosphere at sea level. *Physical Review*, *56*, 10–12.
Mook, W., Bommerson, J., & Staverman, W. (1974). Carbon isotope fractionation between dissolved bicarbonate and gaseous carbon dioxide. *Earth and Planetary Science Letters*, *22*, 169–176.
Muller, R. A. (1977). Radioisotope dating with a cyclotron. *Science*, *196*(4289), 489–494.
Muzikar, P., Elmore, D., & Granger, D. E. (2003). Accelerator mass spectrometry in geologic research. *Bulletin of the Geological Society of America*, *115*(6), 643–654.
Naito, Y. I., Chikaraishi, Y., Ohkouchi, N., Mukai, H., Shibata, Y., Honch, N. V., et al. (2010). Dietary reconstruction of the Okhotsk culture of Hokkaido, Japan, based on nitrogen composition of amino acids: Implications for correction of ^{14}C marine reservoir effects on human bones. *Radiocarbon*, *52*(2), 671–681.
Nakamura, T. (2007). Marine reservoir effect deduced from ^{14}C dates on marine shells and terrestrial remains at archeological sites in Japan. *Nuclear Instruments and Methods in Physics Research, Section B: Beam Interactions with Materials and Atoms*, *259*, 453–459.
Nelson, D., Korteling, R., & Stott, W. (1977). Carbon-14: Direct detection at natural concentrations. *Science*, *198*, 507–508.
Nier, A. O., & Gulbransen, E. A. (1939). Variations in the relative abundance of the carbon isotopes. *Journal of the American Chemical Society*, *61*, 697–698.
Niu, M., Heaton, T. J., Blackwell, P. G., & Buck, C. E. (2013). The Bayesian approach to radiocarbon calibration curve estimation: The IntCal13, Marine13, and SHCal13 methodologies. *Radiocarbon*, *55*(4), 1905–1922.
Nydal, R. (2000). Radiocarbon in the ocean. *Radiocarbon*, *42*(1), 81–98.
O'Connor, S., Ulm, S., Fallon, S. J., Barham, A., & Loch, I. (2010). Pre-bomb marine reservoir variability in the Kimberley region, Western Australia. *Radiocarbon*, *52*(2–3), 1158–1165.
Oeschger, H., Siegenthaler, U., Schotterer, U., & Gugelmann, A. (1975). A box diffusion model to study the carbon dioxide exchange in nature. *Tellus*, *27*(2), 168–192.
Past Interglacials Working Group of PAGES (2016). Interglacials of the last 800,000 years. *Reviews of Geophysics*, *54*, 162–219. https://doi.org/10.1002/2015RG000482
Olsen, J., Ascough, P., Lougheed, B. C., & Rasmussen, P. (2017). Radiocarbon dating in estuarine environments. In K. Weckström, et al. (Eds.), *Applications of paleoenvironmental techniques in estuarine studies* (Vol. 20, pp. 141–170). Dordrecht: Springer.
Olsson, I. (1970). *Radiocarbon variations and absolute chronology: Proceedings of the Twelfth Nobel Symposium Held at the Institute of Physics at Uppsala University*: Wiley-Interscience.
Olsson, I. U. (1980). Content of ^{14}C in marine mammals from Northern Europe. *Radiocarbon*, *22*(3), 662–675.
Olsson, I. U. (1983). Dating non-terrestrial materials. In T. Hackens, W. G. Mook, & H. T. Walterbolk (Eds.), *Proceedings of ^{14}C and archaeology (PACT 8)* (Vol. 8, pp. 277–294). Groningen: PACT publication.

Olsson, I. U. (1996). ^{14}C dates and the reservoir effect. In Van Der Plicht, J., & Punning, J. M. (Eds.), *International Workshop on Isotope-Geochemical Research in the Baltic Region* (Vol. 20, pp. 5–23). Groningen, Netherlands: Centre for Isotope Research Groningen.
Ortlieb, L., Vargas, G., & Saliège, J. F. (2011). Marine radiocarbon reservoir effect along the northern Chile-southern Peru coast (14-24S) throughout the Holocene. *Quaternary Research*, *75*(1), 91–103.
Oschmann, W. (2009). Sclerochronology: Editorial. *International Journal of Earth Sciences*, *98*(1), 1–2.
Owen, B. D. (2002). Marine carbon reservoir age estimates for the Far South Coast of Peru. *Radiocarbon*, *44*(3), 701–708.
Pandow, M., MacKay, C., & Wolfgang, R. (1960). The reaction of atomic carbon with oxygen: Significance for the natural radio-carbon cycle. *Journal of Inorganic and Nuclear Chemistry*, *14*, 153–158.
Pearson, G., & Stuiver, M. (1993). High-precision bidecadal calibration of the radiocarbon time scale, 500–2500 BC. *Radiocarbon*, *35*(1), 25–33.
Petchey, F., & Clark, G. (2010). A marine reservoir correction value (ΔR) for the Palauan Archipelago: Environmental and oceanographic considerations. *The Journal of Island and Coastal Archaeology*, *5*, 236–252. https://doi.org/10.1080/15564890903155935
Petchey, F., Phelan, M., & White, J. (2004). New ΔR values for the Southwest Pacific Ocean. *Radiocarbon*, *46*(2), 1005–1014.
Petchey, F., Anderson, A., Zondervan, A., Ulm, S., & Hogg, A. (2008). New marine ΔR values for the South Pacific Subtropical Gyre region. *Radiocarbon*, *50*(3), 373–397.
Petchey, F., Ulm, S., David, B., McNiven, I. J., Asmussen, B., Tomkins, H., et al. (2012). ^{14}C marine reservoir variability in herbivores and deposit-feeding gastropods from an open coastline, Papua New Guinea. *Radiocarbon*, *54*(3–4), 967–978.
Post, W., Peng, T., Emanuel, W., King, A., Dale, V., & DeAngelis, D. (1990). The global carbon cycle. *American Scientist*, *74*, 310–326.
Povinec, P. P., Litherland, A. E., & von Reden, K. F. (2009). Developments in radiocarbon technologies: From the libby counter to compound-specific AMS analyses. *Radiocarbon*, *51*(1), 45–78.
Price, P. (1989). Heavy-particle radioactivity ($A > 4$). *Annual Review of Nuclear and Particle Science*, *39*, 19–42.
Rakowski, A., Kuc, T., Nakamura, T., & Pazdur, A. (2005). Radiocarbon concentration in urban area. *Geochronometria*, *24*, 63–68.
Raven, J. A., & Falkowski, P. G. (1999). Oceanic sinks for atmospheric CO_2. *Plant, Cell and Environment*, *22*(6), 741–755.
Reimer, P., & Reimer, R. (2006). Marine reservoir corrections and the calibration curve. *Pages News*, *14*(3), 12–13.
Reimer, P., Bard, E., Bayliss, J., Beck, A., Blackwell, J. W., Bronk Ramsey, P. G., et al. (2013). IntCal13 and Marine13 radiocarbon age calibration curves 0–50,000 years cal BP–50,000. *Radiocarbon*, *55*(4), 1869–1887.
Reimer, P., Baillie, M. G. L., Bard, E., Bayliss, A., Beck, J. W., Blackwell, P. G., et al. (2009). IntCal09 and Marine09 radiocarbon age calibration curves, 0–50,000 years cal BP. *Radiocarbon*, *51*(4), 1111–1150.
Reimer, P. J., & Reimer, R. W. (2001). A marine reservoir correction database and on-line interface. *Radiocarbon*, *43*(2A), 461–463.
Reimer, P. J., Baillie, M. G. L., Bard, E., Bayliss, A., Beck, J. W., Bertrand, C. J. H., et al. (2004). IntCal04 terrestrial radiocarbon age calibration 0–26 cal kyr BP. *Radiocarbon*, *46*(3), 1029–1058.
Reimer, R. W., & Reimer, P. J. (2016). An online application for ΔR calculation. *Radiocarbon*, *13*, 1–5. https://doi.org/10.1017/RDC.2016.117
Reynolds, G., Harrison, F., & Salvini, G. (1950). Liquid scintillation counters. *Physical Review*, *78*, 488.
Ritz, S. P., Stocker, T. F., & Muller, S. A. (2008). Modeling the effect of abrupt ocean circulation change on marine reservoir age. *Earth and Planetary Science Letters*, *268*(1–2), 202–211. https://doi.org/10.1016/j.epsl.2008.01.024
Rodgers, K. B., Mikaloff-Fletcher, S. E., Bianchi, D., Beaulieu, C., Galbraith, E. D., Gnanadesikan, A., et al. (2011). Interhemispheric gradient of atmospheric radiocarbon reveals natural variability of Southern Ocean winds. *Climate of the Past*, *7*, 1123–1138.
Rose, H., & Jones, G. (1984). A new kind of natural radioactivity. *Nature*, *307*, 245–247.
Rubin, S. I., & Key, R. M. (2002). Separating natural and bomb-produced radiocarbon in the ocean: The potential alkalinity method. *Global Biogeochemical Cycles*, *16*(4), 1105. https://doi.org/10.1029/2001GB001432
Russell, N. (2011). Marine radiocarbon reservoir effects (MRE) in archaeology: Temporal and spatial changes through the Holocene within the UK coastal environment (Ph.D thesis), University of Glasgow.
Russell, N., Cook, G. T., Ascough, P., Barrett, J. H., & Dugmore, A. (2011). Species specific marine radiocarbon reservoir effect: A comparison of ΔR values between Patella vulgata (limpet) shell carbonate and Gadus morhua (Atlantic cod) bone collagen. *Journal of Archaeological Science*, *38*(5), 1008–1015.
Russell, N., Cook, G. T., Ascough, P. L., Scott, E. M., & Dugmore, A. J. (2011). Examining the inherent variability of ΔR: New methods of presenting ΔR values and implications for MRE studies. *Radiocarbon*, *53*(2), 277–288.
Sarmiento, J. L., Hughes, T. M. C., Stouffer, R. J., & Manabe, S. (1998). Simulated response of the ocean carbon cycle to anthropogenic climate warming. *Nature*, *393*(6682), 245–249.
Sarna-Wojcicki, A. (2000). Tephrochronology. In J. S. Noller, J. M. Sowers, & W. R. Lettis (Eds.), *Quaternary geochronology: Methods and applications* (pp. 357–377). Washington, DC: American Geophysical Union.
Sarnthein, M., Grootes, P. M., Kennett, J. P., & Nadeau, M. J. (2007). ^{14}C reservoir ages show deglacial changes in ocean currents and carbon cycle. In Schmittner, A., Chiang, J., & Hemming, S. (Eds.), *Ocean circulation: Mechanisms and impacts—past and future changes of meridional overturning* (pp. 175–196). Washington, DC: American Geophysical Union.
Shackleton, N. J., Duplessy, J.-C., Arnold, M., Maurice, P., Hall, M. A., & Cartlidge, J. (1988). Radiocarbon age of last glacial Pacific deep water. *Nature*, *335*, 708–711.
Shen, C., Yi, W., Yu, K., Sun, Y., Liu, T., Beer, J., et al. (2004). Holocene megathermal abrupt environmental changes derived from ^{14}C dating of a coral reef at Leizhou Peninsula, South China Sea. *Nuclear Instruments and Methods in Physics Research, Section B: Beam Interactions with Materials and Atoms*, *223–224*, 416–419. https://doi.org/10.1016/j.nimb.2004.04.079
Shishikura, M., Echigo, T., & Kaneda, H. (2007). Marine reservoir correction for the Pacific coast of central Japan using ^{14}C ages of marine mollusks uplifted during historical earthquakes. *Quaternary Research*, *67*(2), 286–291. https://doi.org/10.1016/j.yqres.2006.09.003
Siani, G., Paterne, M., Arnold, M., Bard, E., Métivier, B., Tisnerat, N., & Bassinot, F. (2000). Radiocarbon reservoir ages in the Mediterranean Sea and Black Sea. *Radiocarbon*, *42*(2), 271–280.
Siani, G., Paterne, M., Michel, E., Sulpizio, R., Sbrana, A., Arnold, M., & Haddad, G. (2001). Mediterranean sea surface radiocarbon reservoir age changes since the Last Glacial Maximum. *Science*, *294*(5548), 1917–1920. https://doi.org/10.1126/science.1063649
Siani, G., Michel, E., De Pol-Holz, R., Devries, T., Lamy, F., Carel, M., et al. (2013). Carbon isotope records reveal precise timing of enhanced Southern Ocean upwelling during the last deglaciation. *Nature Communications*, *4*, 2758.
Siegenthaler, U., & Sarmiento, J. L. (1993). Atmospheric carbon dioxide and the ocean. *Nature*, *365*, 119–125.
Sigman, D. M., & Boyle, E. A. (2000). Glacial/interglacial variations in atmospheric carbon dioxide. *Nature*, *407*, 859–869.
Sikes, E. L., & Guilderson, T. P. (2016). Southwest Pacific Ocean surface reservoir ages since the last glaciation: Circulation insights from multiple-core studies. *Paleoceanography*, *31*, 298–310. https://doi.org/10.1002/2015PA002855
Sikes, E. L., Samson, C. R., Guilderson, T. P., & Howard, W. R. (2000). Old radiocarbon ages in the southwest Pacific Ocean during the last glacial period and deglaciation. *Nature*, *405*(6786), 555–559.

Sikes, E. L., Burgess, S. N., Grandpre, R., & Guilderson, T. P. (2008). Assessing modern deep-water ages in the New Zealand region using deep-water corals. *Deep-Sea Research Part I: Oceanographic Research Papers*, *55*(1), 38–49.
Sikes, E. L., Cook, M. S., & Guilderson, T. P. (2016). Reduced deep ocean ventilation in the Southern Pacific Ocean during the last glaciation persisted into the deglaciation. *Earth and Planetary Science Letters*, *438*, 130–138.
Skinner, L., Fallon, S., Waekbroeck, C., Michel, E., & Barker, S. (2010). Ventilation of the deep Southern Ocean and deglacial CO_2 rise. *Science*, *328*, 1147–1151.
Skinner, L., McCave, I. N., Carter, L., Fallon, S., Scrivner, A. E., & Primeau, F. (2015). Reduced ventilation and enhanced magnitude of the deep Pacific carbon pool during the last glacial period. *Earth and Planetary Science Letters*, *411*, 45–52.
Soares, A., & Dias, J. (2006). Coastal upwelling and radiocarbon: Evidence for temporal fluctuations in ocean reservoir effect off Portugal during the Holocene. *Radiocarbon*, *48*(1), 45–60.
Soulet, G. (2015). Methods and codes for reservoir—Atmosphere ^{14}C age offset calculations. *Quaternary Geochronology*, *29*, 97–103.
Soulet, G., Skinner, L., Beaupre, S., & Galy, V. (2016). A note on reporting of reservoir ^{14}C disequilibria and age offsets. *Radiocarbon*, *58*, 205–211.
Southon, J., Noronha, A. L., Cheng, H., Edwards, R. L., & Wang, Y. (2012). A high-resolution record of atmospheric ^{14}C based on Hulu Cave speleothem H82. *Quaternary Science Reviews*, *33*, 32–41.
Southon, J. R., Nelson, D. E., & Vogel, J. S. (1990). A record of past ocean-atmosphere radiocarbon differences from the northeast Pacific. *Paleoceanography*, *5*(2), 197–206.
Southon, J. R., Rodman, A. O., & True, D. (1995). A comparison of marine and terrestrial radiocarbon ages from northern Chile. *Radiocarbon*, *37*(2), 389–393.
Southon, J., & Fedje, D. (2003). A post-glacial record of ^{14} reservoir ages for the British Columbia Coast. *Canadian Journal of Archaeology*, *27*(1), 95–111.
Staubwasser, M., Sirocko, F., Grootes, P. M., & Erlenkeuser, H. (2002). South Asian monsoon climate change and radiocarbon in the Arabian Sea during early and middle Holocene. *Paleoceanography*, *17*(4), 1063. https://doi.org/10.1029/2000PA000608
Stern, J. V., & Lisiecki, L. E. (2013). North Atlantic circulation and reservoir age changes over the past 41,000 years. *Geophysical Research Letters*, *40*, 3693–3697. https://doi.org/10.1002/grl.50679
Stocker, T. F., & Wright, D. G. (1996). Rapid changes in ocean circulation and atmospheric radiocarbon. *Paleoceanography*, *11*(6), 773–795.
Strub, P., Mesías, J., Montecino, V., Rutlant, J., & Salinas, S. (1998). Coastal ocean circulation off western South America. In A. R. Robinson, & K. H. Brink (Eds.), *The sea* (Vol. 11, pp. 273–314). New York: John Wiley.
Stuiver, M. (1961). Variations in radiocarbon concentration and sunspot activity. *Journal of Geophysical Research*, *66*(1), 273–276.
Stuiver, M., & Braziunas, T. F. (1993). Modeling atmospheric ^{14}C influences and ^{14}C ages of marine samples to 10,000 BC. *Radiocarbon*, *35*(1), 137–189.
Stuiver, M., & Braziunas, T. F. (1998). Anthropogenic and solar components of hemispheric ^{14}C. *Geophysical Research Letters*, *25*(3), 329–332.
Stuiver, M., & Polach, H. (1977). Reporting of ^{14}C data. *Radiocarbon*, *19*(3), 355–363.
Stuiver, M., & Quay, P. D. (1981). Atmospheric ^{14}C changes resulting from fossil fuel CO_2 release and cosmic ray flux variability. *Earth and Planetary Science Letters*, *53*, 349–362.
Stuiver, M., & Reimer, P. J. (1986). A computer program for radiocarbon age calibration. *Radiocarbon*, *28*(2B), 1022–1030.
Stuiver, M., & Suess, H. (1966). On the relationship between radiocarbon dates and true sample ages. *Radiocarbon*, *8*, 534–540.
Stuiver, M., Pearson, G., & Braziunas, T. (1986). Radiocarbon age calibration of marine samples back to 9000 cal yr BP. *Radiocarbon*, *28*(2B), 980–1021.
Stuiver, M., Braziunas, T. F., Becker, B., & Kromer, B. (1991). Climatic, solar, oceanic, and geomagnetic influences on late-glacial and Holocene atmospheric $^{14}C/^{12}C$ change. *Quaternary Research*, *35*(1), 1–24. https://doi.org/10.1016/0033-5894(91)90091-I
Stuiver, M., Braziunas, T. F., Grootes, P. M., & Zielinski, G. A. (1997). Is there evidence for solar forcing of climate in the GISP2 oxygen isotope record? *Quaternary Research*, *48*, 259–266.
Stuiver, M., Reimer, P., & Braziunas, T. (1998). High-precision radiocarbon age calibrations for terrestrial and marine samples. *Radiocarbon*, *40*(3), 1127–1151.
Stuiver, M., Reimer, P. J., Bard, E., Beck, J. W., Burr, G. S., Hughen, K. A., et al. (1998). INTCAL98 radiocarbon age calibration, 24,000-0 cal BP. *Radiocarbon*, *40*(3), 1041–1083.
Suess, H. E. (1955). Radiocarbon concentration in modern wood. *Science*, *122*(3166), 415–417.
Sulerzhitzky, L. (1971). Radiocarbon dating of volcanoes *. *Bulletin of Volcanology*, *35*(1), 85–94.
Takahashi, T., Sutherland, S. C., Sweeney, C., Poisson, A., Metzl, N., Tilbrook, B., et al. (2002). Global sea-air CO_2 flux based on climatological surface ocean pCO_2, and seasonal biological and temperature effects. *Deep-Sea Research Part II: Topical Studies in Oceanography*, *49*, 1601–1622.
Takahashi, T., Sutherland, S. C., Wanninkhof, R., Sweeney, C., Feely, R. A., Chipman, D. W., et al. (2009). Climatological mean and decadal change in surface ocean pCO_2, and net sea-air CO_2 flux over the global oceans. *Deep-Sea Research Part II: Topical Studies in Oceanography*, *56*(8-10), 554–577.
Talley, L. D., Pickard, G., Emery, W., & Swift, J. (2011). *Descriptive physical oceanography: An introduction*. Boston: Elsevier Science. p. 560.
Talley, L. (2013). Closure of the global overturning circulation through the Indian, Pacific, and Southern Oceans: Schematics and transports. *Oceanography*, *26*(1), 80–97.
Tans, P. P., De Jong, A. F. M., & Mook, W. G. (1979). Natural atmospheric ^{14}C variation and the Suess effect. *Nature*, *280*, 826–828.
Taylor, N (1992). The role of the ocean in the global carbon cycle. *Weather*, *47*(5), 146–151.
Taylor, R. E. (1987). *Radiocarbon dating: An archaeological perspective* (216 pp.). New York: Academic Press.
Taylor, R. E., & Berger, R. (1967). Radiocarbon content of marine shells from the Pacific Coasts of central and South America. *Science*, *158*(1180-1182), 157–168.
Tobias, S., Weiss, N., & Beer, J. (2004). Long-term prediction of solar activity—A discussion.... *Astronomy & Geophysics*, *3*, 209–216.
Tuniz, C., Kutschera, W., Fink, D., Herzog, G., & Bird, J. (1998). *Accelerator mass spectrometry: Ultrasensitive analysis for global science* (400 pp.). Boca Raton, FL: CRC Press.
Ulm, S. (2002). Marine and estuarine reservoir effects in central Queensland, Australia: Determination of ΔR values. *Geoarchaeology*, *17*, 319–348.
Vogel, J., Fuls, A., & Visser, E. (1993). Pretoria calibration curve for short-lived samples, 1930–3350 BC. *Radiocarbon*, *35*(1), 73–85.
Volk, T., & Hoffert, M. I. (1985). Ocean carbon pumps: Analysis of relative strengths and efficiencies in ocean-driven atmospheric CO_2 changes. *The Carbon Cycle and Atmospheric CO: Natural Variations Archean to Present*, *32*, 99–110.
Vorobyov, A. A., Seleverstov, D. M., Grachov, V. T., Kondurov, I. A., Nikitin, A. M., Smirnov, N. N., & Zalite, Y. K. (1972). Light nuclei from ^{235}U neutron fission. *Physics Letters B*, *40B*(1), 102–104.

Ward, G. K., & Wilson, S. R. (1978). Procedures for comparing and combining radiocarbon age determinations: A critique. *Archaeometry*, *20*(1), 19–31.
Weinstock, B. (1969). Carbon monoxide: Residence time in the atmosphere. *Science*, *166*, 224–225.
Weisler, M., Hua, Q., & Zhao, J. (2009). Late Holocene ^{14}C marine reservoir corrections for Hawaii derived from U-series dated archaeological coral. *Radiocarbon*, *51*(3), 955–968.
Williams, P. M., Oeschger, H., & Kinney, P. (1969). Natural radiocarbon activity of the dissolved organic carbon in the north-east Pacific Ocean. *Nature*, *224*(5216), 256–258.
Williams, R. G., & Follows, M. J. (2011). *Ocean dynamics and the carbon cycle: Principles and mechanisms* (p. 434). Cambridge: Cambridge University Press.
Wündsch, M., Haberzettl, T., Meadows, M. E., Kirsten, K. L., Kasper, T., Baade, J., et al. (2016). The impact of changing reservoir effects on the ^{14}C chronology of a Holocene sediment record from South Africa. *Quaternary Geochronology*, *36*, 148–160.
Yamazaki, T., & Oda, H. (2002). Orbital influence on Earth's magnetic field: 100,000-year periodicity in inclination. *Science (New York, N.Y.)*, *295*, 2435–2438.
Yoneda, M., Kitagawa, H., van der Plicht, J., Uchida, M., Tanaka, A., Uehiro, T., et al. (2000). Pre-bomb marine reservoir ages in the western north Pacific: Preliminary result on Kyoto University collection. *Nuclear Instruments and Methods in Physics Research Section B: Beam Interactions with Materials and Atoms*, *172*(1-4), 377–381.
Zare, R. N. (2012). Analytical chemistry: Ultrasensitive radiocarbon detection. *Nature*, *482*, 312–313.
Zazzo, A., Munoz, O., Badel, E., Béguier, I., Genchi, F., & Marcucci, L. G. (2016). A revised radiocarbon chronology of the Aceramic Shell Midden of Ra's Al-Hamra 6 (Muscat, Sultanate of Oman): Implication for occupational sequence, marine reservoir age, and human mobility. *Radiocarbon*, *58*(02), 383–395.
Zeebe, R., & Wolf-Gladrow, D. (2001). *CO_2 in seawater: Equilibrium, kinetics, isotopes* (p. 360). Amsterdam: Elsevier.
Zito, R., Donahue, D. J., Davis, S. N., Bentley, H. W., & Fritz, P. (1980). Possible subsurface production of carbon-14. *Geophysical Research Letters*, *7*, 235–238. https://doi.org/10.1029/GL007i004p00235